ACKNOWLEDGEMENTS

This work was made possible by the provision of everolimus (RAD001) by Novartis Pharma AG (Basel, Switzerland). We thank Novartis Pharma AG for their kindness. We thank Dr Katsunori Imai and Keisuke Miyake for *in vitro* technical assistance, and Dr Satoshi Ida and Dr Hasta Holrad for *in vivo* technical assistance. The content is solely the responsibility of the authors and does not necessarily represent the official views of the NCI or NIH. The funders had no role in the study design, data collection and analysis, decision to publish, or preparation of the manuscript.

Conflict of interest

The authors declare no conflict of interest.

Supplementary Information accompanies the paper on British Journal of Cancer website (http://www.nature.com/bjc)

REFERENCES

Abraham RT, Gibbons JJ (2007) The mammalian target of rapamycin signaling pathway: twists and turns in the road to cancer therapy. *Clin Cancer Res* **13:** 3109–3114

Antonarakis ES, Carducci MA, Eisenberger MA (2010) Novel targeted therapeutics for metastatic castration-resistant prostate cancer. *Cancer Lett* **291:** 1–13

Awada A, Cardoso F, Fontaine C, Dirix L, De Greve J, Sotiriou C, Steinseifer J, Wouters C, Tanaka C, Zoellner U, Tang P, Piccart M (2008) The oral mTOR inhibitor RAD001 (everolimus) in combination with letrozole in patients with advanced breast cancer: results of a phase I study with pharmacokinetics. *Eur J Cancer* **44:** 84–91

Beuvink I, Boulay A, Fumagalli S, Zilbermann F, Ruetz S, O'Reilly T, Natt F, Hall J, Lane HA, Thomas G (2005) The mTOR inhibitor RAD001 sensitizes tumor cells to DNA-damaged induced apoptosis through inhibition of p21 translation. *Cell* **120:** 747–759

Bianco R, Garofalo S, Rosa R, Damiano V, Gelardi T, Daniele G, Marciano R, Ciardiello F, Tortora G (2008) Inhibition of mTOR pathway by everolimus cooperates with EGFR inhibitors in human tumours sensitive and resistant to anti-EGFR drugs. *Br J Cancer* **98:** 923–930

Bianco R, Melisi D, Ciardiello F, Tortora G (2006) Key cancer cell signal transduction pathways as therapeutic targets. *Eur J Cancer* **42:** 290–294

Bjornsti MA, Houghton PJ (2004) The TOR pathway: a target for cancer therapy. *Nat Rev Cancer* **4:** 335–348

Boone J, Ten Kate FJ, Offerhaus GJ, van Diest PJ, Rinkes IH, van Hillegersberg R (2008) mTOR in squamous cell carcinoma of the oesophagus: a potential target for molecular therapy? *J Clin Pathol* **61:** 909–913

Boulay A, Zumstein-Mecker S, Stephan C, Beuvink I, Zilbermann F, Haller R, Tobler S, Heusser C, O'Reilly T, Stolz B, Marti A, Thomas G, Lane HA (2004) Antitumor efficacy of intermittent treatment schedules with the rapamycin derivative RAD001 correlates with prolonged inactivation of ribosomal protein S6 kinase 1 in peripheral blood mononuclear cells. *Cancer Res* **64:** 252–261

Carmeliet P, Jain RK (2000) Angiogenesis in cancer and other diseases. *Nature* **407:** 249–257

Chan S (2004) Targeting the mammalian target of rapamycin (mTOR): a new approach to treating cancer. *Br J Cancer* **91:** 1420–1424

Coppin C (2010) Everolimus: the first approved product for patients with advanced renal cell cancer after sunitinib and/or sorafenib. *Biologics* **4:** 91–101

Dancey JE (2006) Therapeutic targets: MTOR and related pathways. *Cancer Biol Ther* **5:** 1065–1073

Del Bufalo D, Trisciuoglio D, Scarsella M, D'Amati G, Candiloro A, Iervolino A, Leonetti C, Zupi G (2004) Lonidamine causes inhibition of angiogenesis-related endothelial cell functions. *Neoplasia* **6:** 513–522

Easton JB, Houghton PJ (2006) mTOR and cancer therapy. *Oncogene* **25:** 6436–6446

Enzinger PC, Mayer RJ (2003) Esophageal cancer. *N Engl J Med* **349:** 2241–2252

Fouladi M, Laningham F, Wu J, O'Shaughnessy MA, Molina K, Broniscer A, Spunt SL, Luckett I, Stewart CF, Houghton PJ, Gilbertson RJ, Furman WL (2007) Phase I study of everolimus in pediatric patients with refractory solid tumors. *J Clin Oncol* **25:** 4806–4812

Gridelli C, Rossi A, Morgillo F, Bareschino MA, Maione P, Di Maio M, Ciardiello F (2007) A randomized phase II study of pemetrexed or RAD001 as second-line treatment of advanced non-small-cell lung cancer in elderly patients: treatment rationale and protocol dynamics. *Clin Lung Cancer* **8:** 568–571

Herberger B, Puhalla H, Lehnert M, Wrba F, Novak S, Brandstetter A, Gruenberger B, Gruenberger T, Pirker R, Filipits M (2007) Activated mammalian target of rapamycin is an adverse prognostic factor in patients with biliary tract adenocarcinoma. *Clin Cancer Res* **13:** 4795–4799

Hidalgo M, Rowinsky EK (2000) The rapamycin-sensitive signal transduction pathway as a target for cancer therapy. *Oncogene* **19:** 6680–6686

Hirashima K, Baba Y, Watanabe M, Karashima R, Sato N, Imamura Y, Hiyoshi Y, Nagai Y, Hayashi N, Iyama K, Baba H (2010) Phosphorylated mTOR expression is associated with poor prognosis for patients with esophageal squamous cell carcinoma. *Ann Surg Oncol* **17:** 2486–2493

Hou G, Xue L, Lu Z, Fan T, Tian F, Xue Y (2007) An activated mTOR/p70S6K signaling pathway in esophageal squamous cell carcinoma cell lines and inhibition of the pathway by rapamycin and siRNA against mTOR. *Cancer Lett* **253:** 236–248

Hou G, Zhang Q, Wang L, Liu M, Wang J, Xue L (2010) mTOR inhibitor rapamycin alone or combined with cisplatin inhibits growth of esophageal squamous cell carcinoma in nude mice. *Cancer Lett* **290:** 248–254

Hudes GR (2009) Targeting mTOR in renal cell carcinoma. *Cancer* **115:** 2313–2320

Johnson BE, Jackman D, Janne PA (2007) Rationale for a phase I trial of erlotinib and the mammalian target of rapamycin inhibitor everolimus (RAD001) for patients with relapsed non small cell lung cancer. *Clin Cancer Res* **13:** s4628–s4631

Johnston SR (2006) Clinical efforts to combine endocrine agents with targeted therapies against epidermal growth factor receptor/human epidermal growth factor receptor 2 and mammalian target of rapamycin in breast cancer. *Clin Cancer Res* **12:** 1061–108s

Kapoor A (2009) Inhibition of mTOR in kidney cancer. *Curr Oncol* **16**(Suppl 1)**:** S33–S39

Lane HA, Wood JM, McSheehy PM, Allegrini PR, Boulay A, Brueggen J, Littlewood-Evans A, Maira SM, Martiny-Baron G, Schnell CR, Sini P, O'Reilly T (2009) mTOR inhibitor RAD001 (everolimus) has anti-angiogenic/vascular properties distinct from a VEGFR tyrosine kinase inhibitor. *Clin Cancer Res* **15:** 1612–1622

Ma BB, Lui VW, Hui EP, Lau CP, Ho K, Ng MH, Cheng SH, Tsao SW, Chan AT (2010) The activity of mTOR inhibitor RAD001 (everolimus) in nasopharyngeal carcinoma and cisplatin-resistant cell lines. *Invest New Drugs* **28:** 413–420

Mabuchi S, Altomare DA, Cheung M, Zhang L, Poulikakos PI, Hensley HH, Schilder RJ, Ozols RF, Testa JR (2007) RAD001 inhibits human ovarian cancer cell proliferation, enhances cisplatin-induced apoptosis, and prolongs survival in an ovarian cancer model. *Clin Cancer Res* **13:** 4261–4270

Manegold PC, Paringer C, Kulka U, Krimmel K, Eichhorn ME, Wilkowski R, Jauch KW, Guba M, Bruns CJ (2008) Antiangiogenic therapy with mammalian target of rapamycin inhibitor RAD001 (Everolimus) increases radiosensitivity in solid cancer. *Clin Cancer Res* **14:** 892–900

Menon S, Manning BD (2008) Common corruption of the mTOR signaling network in human tumors. *Oncogene* **27**(Suppl 2)**:** S43–S51

Milella M, Trisciuoglio D, Bruno T, Ciuffreda L, Mottolese M, Cianciulli A, Cognetti F, Zangemeister-Wittke U, Del Bufalo D, Zupi G (2004) Trastuzumab down-regulates Bcl-2 expression and potentiates apoptosis induction by Bcl-2/Bcl-XL bispecific antisense oligonucleotides in HER-2 gene-amplified breast cancer cells. *Clin Cancer Res* **10:** 7747–7756

Mita MM, Mita A, Rowinsky EK (2003) The molecular target of rapamycin (mTOR) as a therapeutic target against cancer. *Cancer Biol Ther* **2:** S169–S177

O'Donnell A, Faivre S, Burris 3rd HA, Rea D, Papadimitrakopoulou V, Shand N, Lane HA, Hazell K, Zoellner U, Kovarik JM, Brock C, Jones S, Raymond E, Judson I (2008) Phase I pharmacokinetic and pharmacodynamic study of the oral mammalian target of rapamycin inhibitor everolimus in patients with advanced solid tumors. *J Clin Oncol* **26:** 1588–1595

Panwalkar A, Verstovsek S, Giles FJ (2004) Mammalian target of rapamycin inhibition as therapy for hematologic malignancies. *Cancer* **100:** 657–666

Scott KL, Kabbarah O, Liang MC, Ivanova E, Anagnostou V, Wu J, Dhakal S, Wu M, Chen S, Feinberg T, Huang J, Saci A, Widlund HR, Fisher DE, Xiao Y, Rimm DL, Protopopov A, Wong KK, Chin L (2009) GOLPH3 modulates mTOR signalling and rapamycin sensitivity in cancer. *Nature* **459:** 1085–1090

Sparks CA, Guertin DA (2010) Targeting mTOR: prospects for mTOR complex 2 inhibitors in cancer therapy. *Oncogene* **29:** 3733–3744

Tabernero J, Rojo F, Calvo E, Burris H, Judson I, Hazell K, Martinelli E, Ramon y Cajal S, Jones S, Vidal L, Shand N, Macarulla T, Ramos FJ, Dimitrijevic S, Zoellner U, Tang P, Stumm M, Lane HA, Lebwohl D, Baselga J (2008) Dose- and schedule-dependent inhibition of the mammalian target of rapamycin pathway with everolimus: a phase I tumor pharmacodynamic study in patients with advanced solid tumors. *J Clin Oncol* **26:** 1603–1610

Tanaka C, O'Reilly T, Kovarik JM, Shand N, Hazell K, Judson I, Raymond E, Zumstein-Mecker S, Stephan C, Boulay A, Hattenberger M, Thomas G, Lane HA (2008) Identifying optimal biologic doses of everolimus (RAD001) in patients with cancer based on the modeling of preclinical and clinical pharmacokinetic and pharmacodynamic data. *J Clin Oncol* **26:** 1596–1602

Wolpin BM, Hezel AF, Abrams T, Blaszkowsky LS, Meyerhardt JA, Chan JA, Enzinger PC, Allen B, Clark JW, Ryan DP, Fuchs CS (2009) Oral mTOR inhibitor everolimus in patients with gemcitabine-refractory metastatic pancreatic cancer. *J Clin Oncol* **27:** 193–198

Workman P, Aboagye EO, Balkwill F, Balmain A, Bruder G, Chaplin DJ, Double JA, Everitt J, Farningham DA, Glennie MJ, Kelland LR, Robinson V, Stratford IJ, Tozer GM, Watson S, Wedge SR, Eccles SA (2010) Guidelines for the welfare and use of animals in cancer research. *Br J Cancer* **102:** 1555–1577

Wouters BG, Koritzinsky M (2008) Hypoxia signalling through mTOR and the unfolded protein response in cancer. *Nat Rev Cancer* **8:** 851–864

Yao JC, Phan AT, Chang DZ, Wolff RA, Hess K, Gupta S, Jacobs C, Mares JE, Landgraf AN, Rashid A, Meric-Bernstam F (2008) Efficacy of RAD001 (everolimus) and octreotide LAR in advanced low- to intermediate-grade neuroendocrine tumors: results of a phase II study. *J Clin Oncol* **26:** 4311–4318

Yee KW, Zeng Z, Konopleva M, Verstovsek S, Ravandi F, Ferrajoli A, Thomas D, Wierda W, Apostolidou E, Albitar M, O'Brien S, Andreeff M, Giles FJ (2006) Phase I/II study of the mammalian target of rapamycin inhibitor everolimus (RAD001) in patients with relapsed or refractory hematologic malignancies. *Clin Cancer Res* **12:** 5165–5173

Yoshioka A, Miyata H, Doki Y, Yasuda T, Yamasaki M, Motoori M, Okada K, Matsuyama J, Makari Y, Sohma I, Takiguchi S, Fujiwara Y, Monden M (2008) The activation of Akt during preoperative chemotherapy for esophageal cancer correlates with poor prognosis. *Oncol Rep* **19:** 1099–1107

British Journal of Cancer (2012) 106, 182–188

www.bjcancer.com

Overexpression of microRNA-223 regulates the ubiquitin ligase FBXW7 in oesophageal squamous cell carcinoma

J Kurashige[1], M Watanabe[1], M Iwatsuki[1], K Kinoshita[1], S Saito[1], Y Hiyoshi[1], H Kamohara[1], Y Baba[1], K Mimori[2] and H Baba[*,1]

[1]*Department of Gastroenterological Surgery, Graduate School of Medical Sciences, Kumamoto University, 1-1-1 Honjo, Kumamoto 860-8556, Japan;* [2]*Department of Surgery, Medical Institute of Bioregulation, Kyushu University, 4546 Tsurumihara, Beppu 874-0838, Japan*

BACKGROUND: F-box and WD repeat domain-containing 7 (FBXW7) is a cell cycle regulatory gene whose protein product ubiquitinates positive cell cycle regulators such as c-Myc, cyclin E, and c-Jun, thereby acting as a tumour-suppressor gene. This study focused on microRNA-223 (miR-223), which is a candidate regulator of *FBXW7* mRNA. The aim of this study was to clarify the clinical significance of miR-223 and FBXW7 in oesophageal squamous cell carcinoma (ESCC) patients, and to elucidate the mechanism by which FBXW7 is regulated by miR-223.

METHODS: The expression levels of miR-223 and the expression of FBXW7 protein was examined using 109 resected specimens to determine the clinicopathological significance. We also investigated the role of miR-223 in the regulation of *FBXW7* expression in ESCC cell lines in an *in vitro* analysis.

RESULTS: We found that miR-223 expression was significantly higher in cancerous tissues than in the corresponding normal tissues. There was a significant inverse relationship between the expression levels of miR-223 and FBXW7 protein. Moreover, patients with high miR-223 expression demonstrated a significantly poorer prognosis than those with low expression. On the basis of a series of gain-of-function and loss-of-function studies *in vitro*, we identified *FBXW7* as a functional downstream target of miR-223.

CONCLUSION: Our present study indicates that high expression of miR-223 had a significant adverse impact on the survival of ESCC patients through repression of the function of FBXW7.

British Journal of Cancer (2012) **106,** 182–188. doi:10.1038/bjc.2011.509 www.bjcancer.com
Published online 22 November 2011

Keywords: microRNA; FBXW7; ubiquitin ligase

F-box and WD repeat domain-containing 7 (FBXW7) is the substrate recognition component of an evolutionarily conserved SCF (complex of SKP1, CUL1, and F-box protein)-type ubiquitin ligase complexes, which has been well characterised and shown to have important roles in regulating the stability of multiple oncoprotein substrates, including cyclin E, c-Myc, Notch, c-Jun, mammalian target of rapamycin, and MCL1 (Nakayama and Nakayama, 2006; Mao *et al*, 2008; Welcker and Clurman, 2008; Inuzuka *et al*, 2011; Wertz *et al*, 2011). Therefore, the altered expression of FBXW7 is recognised to be one of the major causes of carcinogenesis or cancer development. We have previously revealed that loss of *FBXW7* correlated with a poor prognosis in colon cancer (Iwatsuki *et al*, 2010). Similarly, low expression of *FBXW7* has been reported to be significantly associated with poor prognoses in glioma (Bredel *et al*, 2005; Hagedorn *et al*, 2007), gastric cancer (Yokobori *et al*, 2009), and breast cancer (Ibusuki *et al*, 2011). However, significance of downregulation of this molecule in oesophageal squamous cell carcinoma (ESCC) remains unknown.

Recent studies have revealed that microRNAs (miRNA) can act as oncogenes or tumour suppressors during the development and progression of cancers through sequence-specific binding to their mRNA targets (Ambros, 2004; Zamore and Haley, 2005; Meister, 2007). These miRNAs have an important role in a wide variety of complex biological processes, including cellular development and differentiation, but investigations have only begun to clarify their significance in carcinogenesis (Calin *et al*, 2004; Croce and Calin, 2005). Some researchers have noted that alterations in the miRNA expression profile strongly affect the progression of human tumours and the prognosis of the patients (Yanaihara *et al*, 2006; Bloomston *et al*, 2007; Schetter *et al*, 2008; Ueda *et al*, 2010). Although our previous study revealed that miR-21 is significantly overexpressed in ESCC (Hiyoshi *et al*, 2009), there have been few reports concerning the miRNA profiles in ESCC.

It was recently reported that microRNA-223 (miR-223) targets the *FBXW7* mRNA 3′-untranslated region, and that overexpression of miR-223 significantly reduces *FBXW7* mRNA levels, increases endogenous cyclin E protein and activity levels, and increases genomic instability (Xu *et al*, 2010). Nevertheless, to our knowledge, no study has been reported on the relationship between the expression levels of miR-223 and FBXW7 in clinical samples of solid tumours. However, no correlation between miR-223 and FBXW7 has yet been elucidated in ESCC.

In the present study, we examined the correlation between the expression levels of miR-223 and immunohistochemical staining for the FBXW7 protein in 109 consecutive ESCC samples, and we

*Correspondence: Dr H Baba; E-mail: hdobaba@kumamoto-u.ac.jp
Revised 29 September 2011; accepted 28 October 2011; published online 22 November 2011

also investigated the prognostic significance of the expression of miR-223. Moreover, we identified *FBXW7* as a functional downstream target of miR-223 *in vitro*.

PATIENTS AND METHODS

Patients and tissue samples

Primary ESCC tissue samples and samples of matched normal oesophageal epithelium were obtained from 109 patients who underwent oesophageal resection without preoperative treatment in the Department of Gastroenterological Surgery, Kumamoto University Hospital from 2000 to 2007. Written informed consent was obtained from all patients. The clinicopathological characteristics, including age, gender, pathology, differentiation, and tumour-node metastasis classification were available for all patients. Survival was measured from the time of oesophageal resection and death was the endpoint. The patient prognoses were examined in March 2011. The median observation time for survival was 31 months and it ranged from 1 to 132 months. The study was approved by the medical ethics committee of Kumamoto University.

ESCC cell lines

The human ESCC cell lines TE1, TE4, TE6, TE8, TE9, TE10, TE14, and TE15 were provided by the Cell Resource Center for Biomedical Research Institute of Development, Aging and Cancer, Tohoku University, Japan. All cells were grown in RPMI 1640 (Cambrex, East Rutherford, NJ, USA) supplemented with 10% fetal bovine serum (Sigma-Aldrich, St Louis, MO, USA), 2 mmol l^{-1} glutamine, 100 units of penicillin per ml, and 100 μg of streptomycin per ml (Cambrex), and were incubated at 37°C in a humidified chamber supplemented with 5% CO_2.

miRNA isolation

The miRNAs were extracted from formalin-fixed, paraffin-embedded oesophageal tissues using a RecoverAll Total Nucleic Acid Isolation Kit for FFPE (Ambion, Austin, TX, USA), according to the manufacturer's instructions. The purity and concentration of all RNA samples were evaluated by their absorbance ratio at 260/280 nm determined with a NanoDrop ND-1000 spectrophotometer (NanoDrop Technologies, Rockland, DE, USA).

Quantitative real-time reverse transcription-PCR (qRT-PCR)

The expression levels of miR-223 were determined by TaqMan qRT-PCR using TaqMan microRNA assay kits (Ambion, USA) according to the manufacturer's protocols, as described previously (Hiyoshi *et al*, 2009). The miR-223 expression was normalised to that of RNU6B, a small nuclear RNA. The expression levels of *FBXW7* were determined using primers and probes that were designed using the Universal Probe Library (Roche Diagnostics, Mannheim, Germany) following the manufacturer's recommendations. The primer sequences used for real-time PCR were as follows: *FBXW7* forward 5′-AAAGAGTTGTTAGCGGTTCTCG-3′, reverse 5′-CCACATGGATACCATCAAACTG-3′and universal probe #78; *18s rRNA* forward 5′-TGGAGGAGACGTTCCAGTGT-3′, reverse 5′-GATCTGTCCAGGCAGTCCTT-3′ and universal probe #17. All qRT-PCR reactions were run using a LightCycler 480 System II (Roche Diagnostics, USA). The relative amounts of miR-223 and *FBXW7* were measured using the $2^{-\Delta\Delta CT}$ method. All qRT-PCR reactions were performed in triplicate.

Immunohistochemical analysis

The immunohistochemical studies for FBXW7, c-Myc, and c-Jun were performed on formalin-fixed, paraffin-embedded surgical sections obtained from 109 patients with ESCC. Tissue sections of 5 μm thickness were deparaffinized and pre-treated for antigen retrieval by autoclave heating in 10 mM sodium citrate buffer (pH 9.0) for 15 min. These sections were blocked for endogenous peroxidase activity with 3% H_2O_2 in methanol for 60 min and then washed in phosphate-buffered saline. The sections were incubated in primary mouse monoclonal anti-FBXW7 (1:100, Abnova Corporation, Taipei, Taiwan), mouse monoclonal anti-c-Myc (sc-40, 1:100, Santa Cruz Biotechnology, Fremont, CA, USA), or rabbit polyclonal anti-c-Jun (sc-1694, 1:50, Santa Cruz Biotechnology) antibody. Tissue sections were immunohistochemically stained using ENVISION reagents (ENVISION+ Dual Link System-HRP, Dako Cytomation, Glostrup, Denmark). All sections were counterstained with haematoxylin. The staining assessment was independently carried out by two authors (JK and YB) without any information about the patients' clinicopathological characteristics or prognosis.

Transfection of miRNA

The cells were transfected with 20 nM Pre-miR miRNA Precursor Molecule pre-223 (pre-miR-223) and 100 nM anti-miR miRNA inhibitor anti-223 (anti-miR-223) (Applied Biosystems) using the Lipofectamine 2000 transfection reagent (Invitrogen, Carlsbad, CA, USA), according to the manufacturer's instructions. The specificity of the transfection was verified using the Pre-miR miRNA Precursor Molecule Negative Control #1 (control pre-miR) and Anti-miR miRNA Inhibitors Negative Control #1 (control anti-miR) (Applied Biosystems). The expression levels of miR-223 and *FBXW7* were quantified 72 h after transfection, and the cells were used for a western blot analysis.

Western blot analysis

To isolate the proteins, cells harvested from 6-well plates were washed once in phosphate-buffered saline and lysed in lysis buffer (Tris-HCl (pH 7.4) 25 mmol l^{-1}, NaCl 100 mmol l^{-1}, EDTA 2 mmol l^{-1}, Triton X 1%, with 10 μg ml^{-1} aprotinin, 10 μg ml^{-1} leupeptin, and 1 mmol l^{-1} Na_3VO_4, 1 mmol l^{-1} phenylmethylsulfonylfluoride). Each protein sample (15 μg) was resolved by sodium dodecyl sulphate-polyacrylamide gel electrophoresis, transferred onto a polyvinylidene difluoride membrane, and incubated with a monoclonal antibody against c-Myc (sc-40, 1:500, Santa Cruz Biotechnology), c-Jun (sc-1694, 1:500, Santa Cruz Biotechnology) or β-actin (1:2000; Sigma-Aldrich). The signals were detected by incubation with secondary antibodies labelled using the ECL Detection System (GE Healthcare, Little Chalfont, UK).

Statistical analysis

All experiments were repeated at least three times. Continuous variables were expressed as the means ± s.d. The relationship between the expression of miR-223, the FBXW7 protein, and the patient clinicopathological characteristics was analysed using Student's *t*-test or a χ^2-analysis. The overall survival curves were plotted according to the Kaplan-Meier method, and the generalised log-rank test was applied to compare the survival curves. The findings were considered to be significant at a *P*-value <0.05. All statistical analyses were performed using the SPSS v. 13.0 software program (SPSS, Inc., Chicago, IL, USA).

RESULTS

Clinicopathological significance of miR-223 in ESCC patients

The expression levels of miR-223 were examined in 109 ESCC clinical samples using qRT-PCR, with quantified values used to

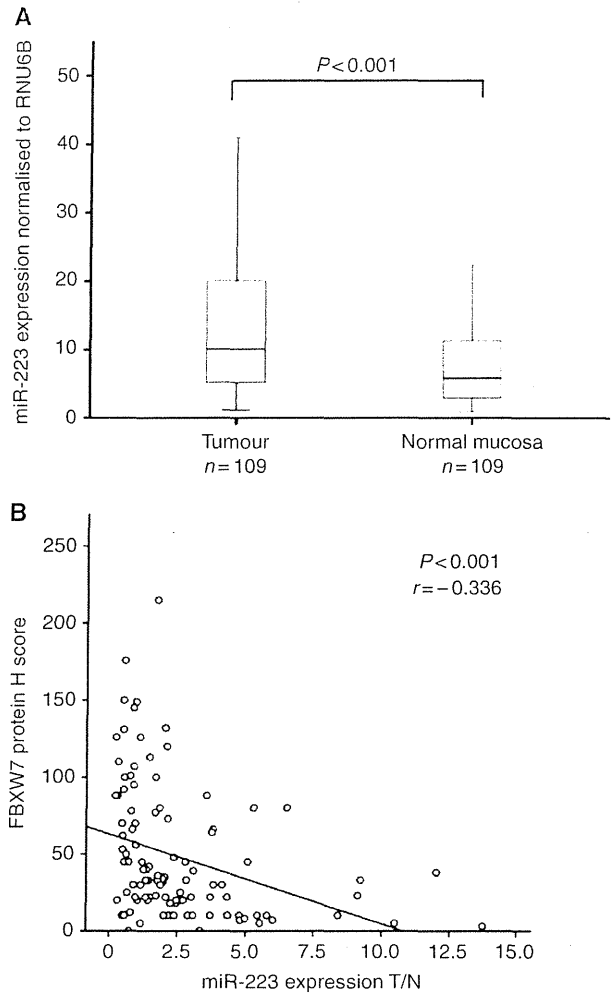

Figure 1 The correlation between the expression of miR-223 and the FBXW7 protein in ESCC patients. (**A**) The expression level of miR-223 in tumour tissue specimens was significantly higher than that in non-tumour tissues ($P<0.001$). (**B**) To evaluate the expression of FBXW7, the complete H score was semiquantitatively calculated (0–300). The relationship between miR-223 and FBXW7 in 109 clinical samples of ESCC indicated an inverse correlation (Pearson correlation, $r=-0.336$; $P<0.01$).

calculate miR-223/U6B ratios. The mean expression levels of miR-223 in cancerous tissue specimens were significantly higher than those in non-cancerous tissues ($P<0.001$; Figure 1A). We divided the 109 ESCC patients into two groups according to the ratio of their cancer/normal tissue expression levels of miR-223, as $\geqslant 1.0$ or <1.0 for the cancer/noncancerous tissues expression levels of miR-223. There were 74 cases (67.9%) in the high miR-223 group and 35 cases (32.1%) in the low miR-223 expression group. The association between the patient clinicopathological characteristics and miR-223 expression is summarised in Table 1. There were significant differences in gender ($P=0.008$), tumour size ($P=0.042$), and depth of tumour invasion ($P=0.030$) between the groups.

The relationship between the expression of miR-223 and immunohistochemical staining for the FBXW7 protein in ESCC tissues

A fragment of the *FBXW7* 3′-untranslated region contained three putative miR-223 binding sites as determined by a computational analysis using miRNA target prediction programs such as Target Scan (http://www.targetscan.org) and miRanda (http://www.microrna.org) (Supplementary Figure 1).

We examined the FBXW7 protein expression level by an immunohistochemical analysis in the samples from ESCC patients. To evaluate the FBXW7 expression, the complete H score was semiquantitatively calculated by summing the products of the percentage of cells stained at a given staining intensity (0–100) and the staining intensity score (0, none; 1, weak; 2, moderate; and 3, intense). We found an inverse correlation between the expression levels of miR-223 and FBXW7 in 109 clinical samples of ESCC. High levels of miR-223 were associated with low FBXW7 expression (Pearson correlation, $r=-0.336$; $P<0.01$; Figure 1B).

Table 1 The miR-223 expression and clinicopathological characteristics of the patients

Factors	Total ($n=109$)	High ($n=74$)	Low ($n=35$)	*P*-value
Age (mean ± s.d.)		66.0 ± 9.5	65.0 ± 8.4	0.967
Sex				0.008*
Male	90	66	24	
Female	19	8	11	
Histological grade				0.821
Well	42	28	14	
Moderate, poor, others	67	46	21	
Size				0.042*
<40 mm (small)	50	29	21	
⩾40 mm (large)	59	45	14	
Depth of tumor invasion				0.030*
T1	46	26	20	
T2/3	63	48	15	
Lymph node metastasis				0.707
Absent	47	31	16	
Present	62	43	19	
Lymphatic invasion				0.617
Absent	43	28	15	
Present	66	46	20	
Venous invasion				0.343
Absent	38	28	10	
Present	71	46	25	
Stage				0.072
I, II	78	49	29	
III, IV	31	25	6	
FBXW7				0.001*
Positive	39	16	23	
Negative	70	58	12	

Abbreviations: moderate = moderately differentiated; poor = poorly differentiated; well = well differentiated. Note: High miR-223 expression group ($n=74$), miR223 (T)/miR223 (N) ⩾ 1.0; low miR-223 expression group ($n=35$), miR-223 (T)/miR-223 (N) < 1.0. *$P<0.05$.

The prognostic significance of miR-223 and FBXW7 in ESCC

An analysis of 5-year overall survival demonstrated that the high miR-223 expression group had a significantly poorer prognosis than the low expression group ($P=0.034$; Figure 2A). Similarly, the negative FBXW7 group had a significantly poorer prognosis of 5-year overall survival than the positive group ($P=0.023$; Figure 2B). In a univariate Cox regression analysis, compared with the low miR-223 expression group, the high miR-223 expression group experienced a significantly higher overall mortality (hazard

ratio 2.272; 95% confidence interval, 1.099–4.695; $P=0.027$; Table 2). In the univariate analysis, other significant prognostic factors for cancer-specific survival included lymph node metastasis ($P=0.008$), lymphatic invasion ($P=0.002$), and FBXW7 expression ($P=0.023$). In a multivariate Cox regression analysis for overall survival, including age at operation, N status, venous invasion, and miR-223 expression, high miR-223 expression was revealed to be an independent prognostic factor (multivariate hazard ratio 2.425; 95% confidence interval, 1.205–4.878; $P=0.013$; Table 2).

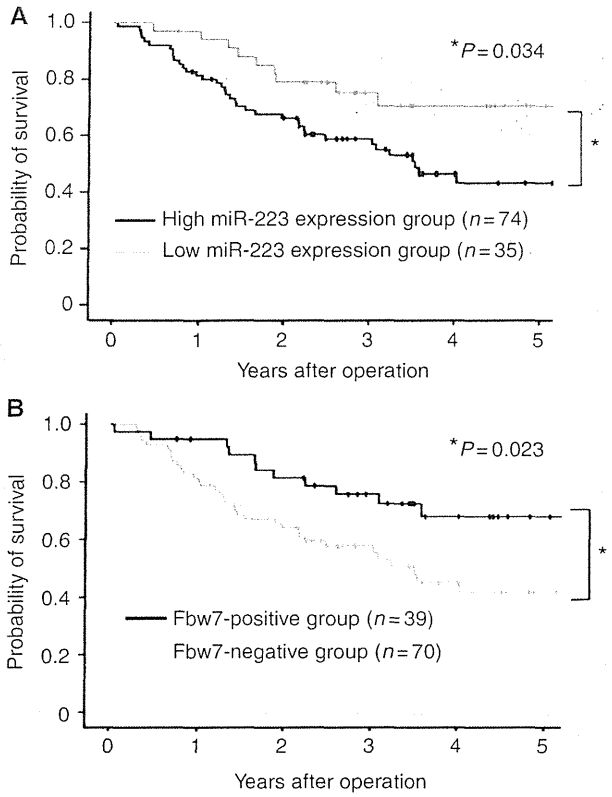

Figure 2 *Kaplan–Meier curves according to the miR-223 and FBXW7 status.* (**A**) The overall survival curves are presented according to the expression level of miR-223 in ESCC patients. Patients with high miR-223 expression had a poorer prognosis than those with low expression (log-rank (Mantel–Cox) test; $P=0.034$). (**B**) The overall survival curves according to the FBXW7 expression level in ESCC patients. The negative FBXW7 group had a significantly poorer prognosis for 5-year overall survival than the positive group ($P=0.023$).

The clinicopathological significance of FBXW7

We used the H score to evaluate the FBXW7 expression level and defined a final staining score of >50 as positive for FBXW7. Among the 109 ESCC patients, 39 patients (35.8%) showed positive staining for FBXW7. The associations between the patient clinicopathological characteristics and FBXW7 are summarised in Supplementary Table 1. There were no significant differences in the patient clinicopathological characteristics.

The relationship between FBXW7, and c-Myc and c-Jun in ESCC tissues

We examined the association between the FBXW7 protein expression, and c-Myc and c-Jun protein expression levels in the

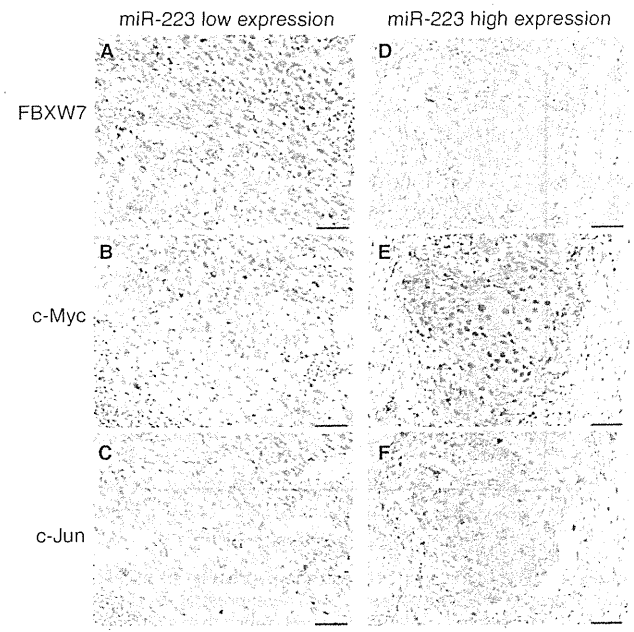

Figure 3 *The relationship between the expression of miR-223, and FBXW7, c-Myc, and c-Jun proteins in ESCC patients.* (**A–C**) In the miR-223-low expression cases, the FBXW7 protein was expressed at a high level, whereas the levels of the c-Myc and c-Jun proteins were below the limit of detection in the same tissue sections. (**D–F**) In contrast, in the miR-223-high expression cases, the FBXW7 protein was expressed at a low level, and there was strong expression of the c-Myc and c-Jun proteins. (× 200 original magnification, scale bar: 50 μm).

Table 2 The results of univariate and multivariate analyses for overall survival (Cox proportional regression model)

	Univariate analysis			Multivariate analysis		
Factors	**HR**	**95% CI**	***P*-value**	**HR**	**95% CI**	***P*-value**
Age (64</65>)	1.559	0.887–2.739	0.123	1.95	1.084–3.506	0.026*
Sex (male/female)	0.622	0.265–1.4682	0.276	—	—	—
T1/2,3	1.386	0.719–2.673	0.33	—	—	—
Tumor size (40 mm<, 40 mm≥)	1.389	0.791–2.438	0.253	—	—	—
Lympha node metastasis (absent/ present)	2.345	1.254–4.385	0.008*	2.371	1.250–4.499	0.008*
Stage I, II/III, IV	1.947	1.079–3.513	0.027*	—	—	—
Venous invasion (absent/present)	1.66	0.892–3.089	0.11	1.42	0.747–2.699	0.285
Lymphatic invasion (absent/present)	2.978	1.513–5.862	0.002*	—	—	—
FBXW7 expression (positive/negative)	2.106	1.094–4.057	0.023*	—	—	—
miR223 expression (low/high)	2.272	1.099–4.695	0.027*	2.425	1.205–4.878	0.013*

Abbreviations: CI = confidence interval; HR = hazard ratio. *$P<0.05$.

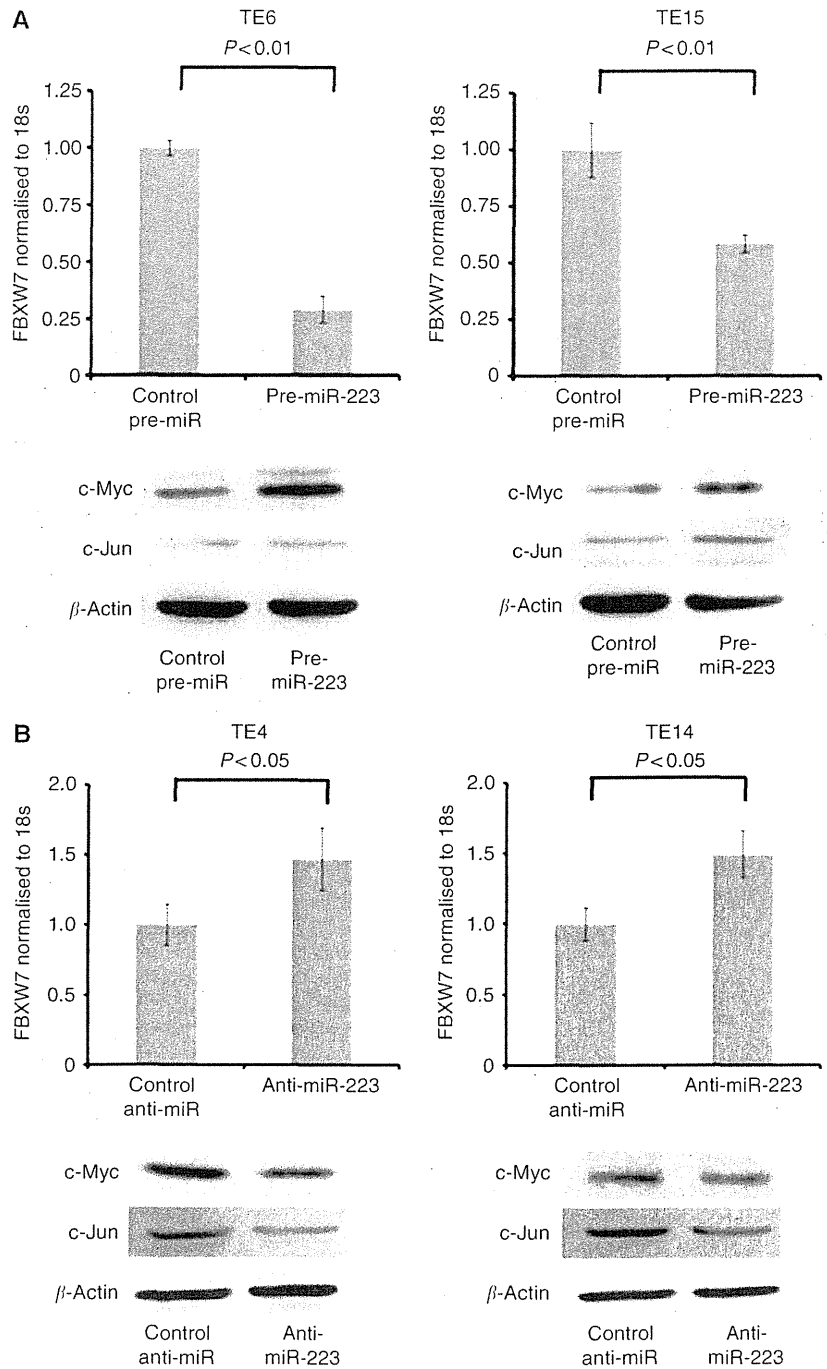

Figure 4 miR-223 gain-of-function and loss-of-function studies in ESCC cell lines. (**A**) The expression of the FBXW7 mRNA was significantly suppressed by transfection of cells with pre-miR-223, as confirmed by qRT–PCR in TE6 and TE15 cells. Furthermore, the expression of the c-Myc and c-Jun proteins was enhanced by treatment with pre-miR-223 as determined by a western blotting analysis. (**B**) In contrast, the FBXW7 mRNA level was significantly increased by transfection of TE4 and TE14 cells with anti-miR-223, and the c-Myc and c-Jun proteins were deregulated.

samples from ESCC patients. When the FBXW7 protein was expressed at high levels, the expression levels of the c-Myc and c-Jun proteins were below the limits of detection in the miR-223 low expression cases (Figures 3A–C). In contrast, in cases with low FBXW7 protein expression, a strong expression of the c-Myc and c-Jun proteins was noted in the cases with high miR-223 expression (Figures 3D–F).

There is an inverse correlation between miR-223 and *FBXW7 in vitro*

Across all the eight cell lines tested, there was a significant inverse correlation between the expression levels of miR-223 and *FBXW7* mRNA (Pearson correlation, $r = -0.855$; $P = 0.007$; Supplementary Figure 2). TE6 and TE15 cells were used to evaluate the effects of

the upregulation of miR-223, and TE4 and TE14 cells were used to examine how the downregulation of miR-223 affected the *FBXW7* expression. *FBXW7* mRNA significantly decreased when cells were transfected with pre-miR-223, compared with those transfected with the negative control (Figure 4A).

Furthermore, we found that the protein expression levels of c-Myc and c-Jun were enhanced after pre-miR-223 treatment by a western blot analysis. In contrast, the TE4 and TE14 cells transfected with anti-miR-223 showed a decrease in the miR-223 expression, compared with the negative control-treated cells. The *FBXW7* mRNA level was significantly increased in the cells transfected with anti-miR-223, compared with those transfected with the negative control, and the protein expression levels of c-Myc and c-Jun were deregulated in these cells (Figure 4B).

DISCUSSION

In our present study, we found that miR-223 was significantly overexpressed in human ESCC tissue compared with the corresponding normal tissue ($P<0.001$), and that the patients with a high miR-223 expression had a significantly poorer prognosis than those with a low expression ($P=0.034$). We also provide evidence that a negative association exists between the expression of miR-223 and the FBXW7 protein in ESCC patients (Pearson correlation, $r=-0.336$; $P<0.01$), and revealed that the miR-223 expression responds to alterations in the c-Myc and c-Jun protein levels as regulated by the FBXW7 pathway *in vitro*. These findings suggested that the overexpression of miR-223 correlates with the poor prognosis of ESCC, possibly because of repression of the function of the FBXW7 protein.

Loss of FBXW7 function is known to be associated with the dysregulation of several cell cycle regulators, including cyclin E and c-Myc (Welcker *et al*, 2003). In oesophagaeal cancer, amplification and overexpression of these regulators has been thoroughly investigated, and their clinical significance has been reported. Cyclin E, a maintainer of the cell cycle restriction point, is significantly overexpressed in mucosal invasive ESCC compared with normal mucosa (Ohbu *et al*, 2001). The amplification of c-Myc was more frequently found in advanced stages of ESCC than in early stages (Bitzer *et al*, 2003). Therefore, the regulation of FBXW7 may have an important role in the carcinogenesis and progression of ESCC. In this study, there was an inverse correlation between FBXW7, and c-Myc and c-Jun in ESCC samples as indicated by an immunohistochemical analysis. Moreover, an *in vitro* assay demonstrated that there was a decrease in the *FBXW7* expression when miR-223 was overexpressed, which gave rise to an abnormal accumulation of the c-Myc and c-Jun proteins.

miR-223 has been recently reported to have a potential role in tumourigenesis through repressing the function of FBXW7, and the overexpression of miR-223 has been shown to significantly reduce the *FBXW7* mRNA levels, while increasing both the endogenous cyclin E protein and activity levels, as well as genomic instability (Xu *et al*, 2010). Moreover, a recent report identified miR-223 as an E2F1 transcriptional target (Pulikkan *et al*, 2010), and E2F1 and miR-223 comprised an autologous negative feedback loop. These facts indicate that miR-223 is one of the key players in cell cycle regulation at the G1–S transition. In addition, miR-223 has been reported to act as an oncogene in several solid tumours, including gastric, ovarian, and bladder cancers (Gottardo *et al*, 2007; Laios *et al*, 2008; Petrocca *et al*, 2008). Moreover, in gastric cancer, the expression level of miR-223 was reported to be a prognostic marker (Li *et al*, 2010). On the other hand, there has been another report suggesting that miR-223 acts as a tumour suppressor by directly targeting Stathmin1 to stimulate the development and progression of hepatocellular carcinoma (Wong *et al*, 2008). In addition, Li *et al* (2011) revealed the oncogene Artemin to be a target of miR-223 and the overexpression of miR-223 decreased the migration and invasion of oesophageal carcinoma cells. Therefore, on the basis of their findings, miR-223 may have a tumour-suppressor function in oesophageal carcinoma. However, in the current study, on the basis of an investigation of 109 ESCC clinical samples, we showed that miR-223 was significantly overexpressed in the tumour compared with the corresponding normal tissue. We also found that the overexpression of miR-223 correlated with tumour advancement and a poor prognosis. Moreover, in a series of gain-of-function and loss-of-function investigations, we found that these effects may be due to the downregulation of the tumour-suppressor FBXW7, which was targeted by miR-223. The decrease in the expression of *FBXW7* resulting from the overexpression of miR-223 gave rise to the abnormal accumulation of c-Myc and c-Jun proteins. It is well known that one miRNA can regulate many targets and, therefore, it may be possible that the same miRNA may have opposite roles in the progression of cancer in different tissues (Shenouda and Alahari, 2009). As miR-223 also targets other genes, some are oncogenes whereas others are tumour-suppressor genes, further analyses are needed to elucidate the full spectrum of miR-223 functions.

Although we suggested that miR-223 regulates FBXW7, 16 out of 74 samples with high miR-223 expression still showed FBXW7 expression and 12 out of 35 samples with low miR-223 expression did not show FBXW7 as shown in Table 1. The relationship between miR-223 and FBXW7 was therefore not completely inverse. To explain this finding, we speculate that not only miR-223 but also various other mechanisms, have effects on the expression of FBXW7, such as epigenetic transcriptional regulation (Gu *et al*, 2008), the loss of genetic alteration (Iwatsuki *et al*, 2010), the status of *p53* mutation (Yokobori *et al*, 2009), or the regulation by other miRs (miR-25, 27a, 92a) (Xu *et al*, 2010).

In conclusion, the present study at first indicates that a high expression level of miR-223 had a significant adverse impact on the survival of ESCC patients through repression of the function of FBXW7.

ACKNOWLEDGEMENTS

This work was supported in part by the following grants and foundations: Japan Society for the Promotion of Science (JSPS) Grant-in-Aid for Scientific Research; grant numbers 23791550, Takeda Science Foundation 2010, Okukubo Memorial Fund for Medical Research in Kumamoto University School of Medicine 2010, Uehara Memorial Foundation 2010, YOKOYAMA Foundation for Clinical Pharmacology 2011.

Supplementary Information accompanies the paper on British Journal of Cancer website (http://www.nature.com/bjc)

REFERENCES

Ambros V (2004) The functions of animal microRNAs. *Nature* **431**(7006): 350–355

Bitzer M, Stahl M, Arjumand J, Rees M, Klump B, Heep H, Gabbert HE, Sarbia M (2003) C-myc gene amplification in different stages of oesophageal squamous cell carcinoma: prognostic value in relation to treatment modality. *Anticancer Res* **23**(2B): 1489–1493

Bloomston M, Frankel WL, Petrocca F, Volinia S, Alder H, Hagan JP, Liu CG, Bhatt D, Taccioli C, Croce CM (2007) MicroRNA expression

patterns to differentiate pancreatic adenocarcinoma from normal pancreas and chronic pancreatitis. *JAMA* **297**(17): 1901–1908

Bredel M, Bredel C, Juric D, Harsh GR, Vogel H, Recht LD, Sikic BI (2005) Functional network analysis reveals extended gliomagenesis pathway maps and three novel MYC-interacting genes in human gliomas. *Cancer Res* **65**(19): 8679–8689

Calin GA, Liu CG, Sevignani C, Ferracin M, Felli N, Dumitru CD, Shimizu M, Cimmino A, Zupo S, Dono M, Dell'Aquila ML, Alder H, Rassenti L, Kipps TJ, Bullrich F, Negrini M, Croce CM (2004) MicroRNA profiling reveals distinct signatures in B cell chronic lymphocytic leukemias. *Proc Natl Acad Sci USA* **101**(32): 11755–11760

Croce CM, Calin GA (2005) miRNAs, cancer, and stem cell division. *Cell* **122**(1): 6–7

Gottardo F, Liu CG, Ferracin M, Calin GA, Fassan M, Bassi P, Sevignani C, Byrne D, Negrini M, Pagano F, Gomella LG, Croce CM, Baffa R (2007) Micro-RNA profiling in kidney and bladder cancers. *Urol Oncol* **25**(5): 387–392

Gu Z, Mitsui H, Inomata K, Honda M, Endo C, Sakurada A, Sato M, Okada Y, Kondo T, Horii A (2008) The methylation status of FBXW7 beta-form correlates with histological subtype in human thymoma. *Biochem Biophys Res Commun* **377**(2): 685–688

Hagedorn M, Delugin M, Abraldes I, Allain N, Belaud-Rotureau MA, Turmo M, Prigent C, Loiseau H, Bikfalvi A, Javerzat S (2007) FBXW7/hCDC4 controls glioma cell proliferation *in vitro* and is a prognostic marker for survival in glioblastoma patients. *Cell Div* **2**: 9

Hiyoshi Y, Kamohara H, Karashima R, Sato N, Imamura Y, Nagai Y, Yoshida N, Toyama E, Hayashi N, Watanabe M, Baba H (2009) MicroRNA-21 regulates the proliferation and invasion in esophageal squamous cell carcinoma. *Clin Cancer Res* **15**(6): 1915–1922

Ibusuki M, Yamamoto Y, Shinriki S, Ando Y, Iwase H (2011) Reduced expression of ubiquitin ligase FBXW7 mRNA is associated with poor prognosis in breast cancer patients. *Cancer Sci* **102**(2): 439–445

Inuzuka H, Shaik S, Onoyama I, Gao D, Tseng A, Maser RS, Zhai B, Wan L, Gutierrez A, Lau AW, Xiao Y, Christie AL, Aster J, Settleman J, Gygi SP, Kung AL, Look T, Nakayama KI, DePinho RA, Wei W (2011) SCF(FBW7) regulates cellular apoptosis by targeting MCL1 for ubiquitylation and destruction. *Nature* **471**(7336): 104–109

Iwatsuki M, Mimori K, Ishii H, Yokobori T, Takatsuno Y, Sato T, Toh H, Onoyama I, Nakayama KI, Baba H, Mori M (2010) Loss of FBXW7, a cell cycle regulating gene, in colorectal cancer: clinical significance. *Int J Cancer* **126**(8): 1828–1837

Laios A, O'Toole S, Flavin R, Martin C, Kelly L, Ring M, Finn SP, Barrett C, Loda M, Gleeson N, D'Arcy T, McGuinness E, Sheils O, Sheppard B, O'Leary J (2008) Potential role of miR-9 and miR-223 in recurrent ovarian cancer. *Mol Cancer* **7**: 35

Li S, Li Z, Guo F, Qin X, Liu B, Lei Z, Song Z, Sun L, Zhang HT, You J, Zhou Q (2011) miR-223 regulates migration and invasion by targeting Artemin in human esophageal carcinoma. *J Biomed Sci* **18**: 24

Li X, Zhang Y, Ding J, Wu K, Fan D (2010) Survival prediction of gastric cancer by a seven-microRNA signature. *Gut* **59**(5): 579–585

Mao JH, Kim IJ, Wu D, Climent J, Kang HC, DelRosario R, Balmain A (2008) FBXW7 targets mTOR for degradation and cooperates with PTEN in tumor suppression. *Science* **321**(5895): 1499–1502

Meister G (2007) miRNAs get an early start on translational silencing. *Cell* **131**(1): 25–28

Nakayama KI, Nakayama K (2006) Ubiquitin ligases: cell-cycle control and cancer. *Nat Rev Cancer* **6**(5): 369–381

Ohbu M, Kobayashi N, Okayasu I (2001) Expression of cell cycle regulatory proteins in the multistep process of oesophageal carcinogenesis: stepwise over-expression of cyclin E and p53, reduction of p21(WAF1/CIP1) and dysregulation of cyclin D1 and p27(KIP1). *Histopathology* **39**(6): 589–596

Petrocca F, Visone R, Onelli MR, Shah MH, Nicoloso MS, de Martino I, Iliopoulos D, Pilozzi E, Liu CG, Negrini M, Cavazzini L, Volinia S, Alder H, Ruco LP, Baldassarre G, Croce CM, Vecchione A (2008) E2F1-regulated microRNAs impair TGFbeta-dependent cell-cycle arrest and apoptosis in gastric cancer. *Cancer Cell* **13**(3): 272–286

Pulikkan JA, Dengler V, Peramangalam PS, Peer Zada AA, Muller-Tidow C, Bohlander SK, Tenen DG, Behre G (2010) Cell-cycle regulator E2F1 and microRNA-223 comprise an autoregulatory negative feedback loop in acute myeloid leukemia. *Blood* **115**(9): 1768–1778

Schetter AJ, Leung SY, Sohn JJ, Zanetti KA, Bowman ED, Yanaihara N, Yuen ST, Chan TL, Kwong DL, Au GK, Liu CG, Calin GA, Croce CM, Harris CC (2008) MicroRNA expression profiles associated with prognosis and therapeutic outcome in colon adenocarcinoma. *JAMA* **299**(4): 425–436

Shenouda SK, Alahari SK (2009) MicroRNA function in cancer: oncogene or a tumor suppressor? *Cancer Metastasis Rev* **28**(3–4): 369–378

Ueda T, Volinia S, Okumura H, Shimizu M, Taccioli C, Rossi S, Alder H, Liu CG, Oue N, Yasui W, Yoshida K, Sasaki H, Nomura S, Seto Y, Kaminishi M, Calin GA, Croce CM (2010) Relation between microRNA expression and progression and prognosis of gastric cancer: a microRNA expression analysis. *Lancet Oncol* **11**(2): 136–146

Welcker M, Clurman BE (2008) FBW7 ubiquitin ligase: a tumour suppressor at the crossroads of cell division, growth and differentiation. *Nat Rev Cancer* **8**(2): 83–93

Welcker M, Singer J, Loeb KR, Grim J, Bloecher A, Gurien-West M, Clurman BE, Roberts JM (2003) Multisite phosphorylation by Cdk2 and GSK3 controls cyclin E degradation. *Mol Cell* **12**(2): 381–392

Wertz IE, Kusam S, Lam C, Okamoto T, Sandoval W, Anderson DJ, Helgason E, Ernst JA, Eby M, Liu J, Belmont LD, Kaminker JS, O'Rourke KM, Pujara K, Kohli PB, Johnson AR, Chiu ML, Lill JR, Jackson PK, Fairbrother WJ, Seshagiri S, Ludlam MJ, Leong KG, Dueber EC, Maecker H, Huang DC, Dixit VM (2011) Sensitivity to antitubulin chemotherapeutics is regulated by MCL1 and FBW7. *Nature* **471**(7336): 110–114

Wong QW, Lung RW, Law PT, Lai PB, Chan KY, To KF, Wong N (2008) MicroRNA-223 is commonly repressed in hepatocellular carcinoma and potentiates expression of Stathmin1. *Gastroenterology* **135**(1): 257–269

Xu Y, Sengupta T, Kukreja L, Minella AC (2010) MicroRNA-223 regulates cyclin E activity by modulating expression of F-box and WD-40 domain protein 7. *J Biol Chem* **285**(45): 34439–34446

Yanaihara N, Caplen N, Bowman E, Seike M, Kumamoto K, Yi M, Stephens RM, Okamoto A, Yokota J, Tanaka T, Calin GA, Liu CG, Croce CM, Harris CC (2006) Unique microRNA molecular profiles in lung cancer diagnosis and prognosis. *Cancer Cell* **9**(3): 189–198

Yokobori T, Mimori K, Iwatsuki M, Ishii H, Onoyama I, Fukagawa T, Kuwano H, Nakayama KI, Mori M (2009) p53-Altered FBXW7 expression determines poor prognosis in gastric cancer cases. *Cancer Res* **69**(9): 3788–3794

Zamore PD, Haley B (2005) Ribo-gnome: the big world of small RNAs. *Science* **309**(5740): 1519–1524

Thrombospondin-1 Is a Novel Negative Regulator of Liver Regeneration After Partial Hepatectomy Through Transforming Growth Factor-beta1 Activation in Mice

Hiromitsu Hayashi,[1] Keiko Sakai,[1] Hideo Baba,[2] and Takao Sakai[1,3]

The matricellular protein, thrombospondin-1 (TSP-1), is prominently expressed during tissue repair. TSP-1 binds to matrix components, proteases, cytokines, and growth factors and activates intracellular signals through its multiple domains. TSP-1 converts latent transforming growth factor-beta1 (TGF-β1) complexes into their biologically active form. TGF-β plays significant roles in cell-cycle regulation, modulation of differentiation, and induction of apoptosis. Although TGF-β1 is a major inhibitor of proliferation in cultured hepatocytes, the functional requirement of TGF-β1 during liver regeneration remains to be defined *in vivo*. We generated a TSP-1-deficient mouse model of a partial hepatectomy (PH) and explored TSP-1 induction, progression of liver regeneration, and TGF-β-mediated signaling during the repair process after hepatectomy. We show here that TSP-1-mediated TGF-β1 activation plays an important role in suppressing hepatocyte proliferation. TSP-1 expression was induced in endothelial cells (ECs) as an immediate early gene in response to PH. TSP-1 deficiency resulted in significantly reduced TGF-β/Smad signaling and accelerated hepatocyte proliferation through down-regulation of p21 protein expression. TSP-1 induced in ECs by reactive oxygen species (ROS) modulated TGF-β/Smad signaling and proliferation in hepatocytes *in vitro*, suggesting that the immediately and transiently produced ROS in the regenerating liver were the responsible factor for TSP-1 induction. *Conclusions:* We have identified TSP-1 as an inhibitory element in regulating liver regeneration by TGF-β1 activation. Our work defines TSP-1 as a novel immediate early gene that could be a potential therapeutic target to accelerate liver regeneration. (HEPATOLOGY 2012;55:1562-1573)

Cell proliferation is part of the wound-healing response and plays a central role in regeneration after tissue damage. It is crucial to advance our understanding of the molecular mechanisms underlying tissue regeneration and to develop a novel strategy to enhance the regenerative process. Such knowledge, in turn, would yield clinical benefits, such as decreased morbidity and mortality. Partial hepatectomy (PH) is a well-established model system in rodents for studying the molecular mechanisms of liver regeneration. PH triggers activation of the immediate early genes (i.e., genes that are rapidly, but transiently, activated) within approximately the first 4 hours,[1] and thereby hepatocytes reenter the cell-division cycle. Immediate early genes encode proteins that regulate later phases in G_1 and play an important role in cell growth in the regenerating liver.[1,2] The process of liver regeneration after hepatectomy is coordinated by both pro- and antiproliferative factors. Transforming growth factor-beta1 (TGF-β1) is a potent inhibitor of mitogen-stimulated DNA synthesis in cultured hepatocytes.[3] Therefore, it has been thought that TGF-β1 is a potent candidate to

Abbreviations: BrdU, 5-bromo-2-deoxyuridine; CD, cluster of differentiation; CM, conditioned media; ECs, endothelial cells; Erk1/2, extracellular signal-related kinase 1 and 2; HSC, hepatic stellate cell; HUVEC, human umbilical vein endothelial cell; ICC, immunocytochemistry; IF, immunofluorescence; IHC, immunohistochemical; MDA, malondialdehyde; mRNA, messenger RNA; NAC, N-acetylcysteine; PAI-1, plasminogen activator inhibitor-1; PECAM-1, platelet/endothelial cell adhesion molecule-1; PCR, polymerase chain reaction; PH, partial hepatectomy; PI3K, phosphatidylinositide 3-kinase; (PI3K ROS, reactive oxygen species; α-SMA, alpha smooth muscle actin; STAT3, signal transducer and activator of transcription 3; TSP-1, thrombospondin-1; TGF-β1, transforming growth factor-β1; TUNEL, terminal deoxynucleotidyl transferase dUTP nick end labeling; VEGFR, vascular endothelial growth factor-A receptor; WT, wild type.

From the [1]Department of Biomedical Engineering, Lerner Research Institute, Cleveland Clinic, Cleveland, OH; [2]Department of Gastroenterological Surgery, Graduate School of Medical Sciences, Kumamoto University, Kumamoto, Japan; and [3]Orthopedic and Rheumatologic Research Center, Cleveland Clinic, Cleveland, OH.

Received August 12, 2011; accepted November 1, 2011.

This work was supported by the National Institutes of Health (grant no.: R01 DK074538; to T.S.) and the Byotai Taisha Research Foundation and Uehara Memorial Foundation, Japan (to H.H.).

limit or stop liver regeneration after PH.[4] Because TGF-β is synthesized and secreted as a latent complex, the important step in regulating its biological activity is the conversion of the latent form into the active one. However, the contribution of TGF-β to the liver's regenerative response after PH is still poorly understood. *TGF-β1* messenger RNA (mRNA) induction occurs within 4 hours, and levels of TGF-β1 remain elevated until 72 hours after PH.[5,6] In sharp contrast, in the model of complete lack of TGF-β signaling using hepatocyte-specific *TGF-β type II receptor* knockout mice, the lack of TGF-β signaling does not result in prolonged hepatocyte proliferation; rather, only transiently up-regulated proliferation of hepatocytes is shown in the later phase after hepatectomy, with a peak at ~36 hours.[7] These differences raise an open question about whether locally activated TGF-β1 is indeed essential for the inhibition of hepatocyte proliferation *in vivo*. Furthermore, the time course of locally activated TGF-β1 and its activation mechanism after PH still remain largely unknown.

The matricellular protein, thrombospondin-1 (TSP-1), was first shown as a component of the α-granule in platelets and can act as a major activator of latent TGF-β1.[8,9] TSP-1 is induced in response to tissue damage or stress and plays a role as a transient component of extracellular matrix during tissue repair.[8,10,11] However, the roles of TSP-1 and of TSP-1/TGF-β1 interdependence during liver regeneration have not yet been addressed. We hypothesize that the initiation of local TGF-β activation occurs much earlier after PH, and TSP-1 plays a critical role in this process. Here, using a TSP-1-deficient mouse model, we investigated whether TSP-1 would be a suitable molecular target for accelerating liver regeneration after PH.

Materials and Methods

Mutant Mice and Animal Studies. TSP-1-null mice were kindly provided by Dr. Jack Lawler (Beth Israel Deaconess Medical Center, Boston, MA).[12] Male wild-type (WT) and TSP-1-null mice, at 8-12 weeks old (C57BL/6 background), were used for the experiments. The two anterior lobes (i.e., median and left lateral lobes), which comprise 70% of liver weight, were resected, whereas the caudate and right lobes were left intact. This study was approved by the institutional animal care and use committee.

Immunostaining and Western Blotting. For histological analyses, liver samples (the same lobe from each mouse) were either directly frozen in OCT compound (Tissue-Tek; Sakura Finetek, Tokyo, Japan) or fixed overnight in 4% paraformaldehyde in phosphate-buffered saline (pH 7.2) and dehydrated in a graded alcohol series and embedded in paraffin. Then, the materials were sectioned at a thickness of 5 μm. Immunofluorescence (IF) and immunohistochemical (IHC) staining was performed as described previously.[13] The negative control staining was performed without the addition of primary antibody. Immunostained slides were viewed under a Leica DM 5500B microscopic system (Leica Microsystems, Buffalo Grove, IL). A minimum of 10 different images were randomly selected, and the data shown are representative of the results observed. Western blotting analysis was performed as described previously.[13] The same lobe from each mouse was used for protein isolation and subsequent analysis. ImageJ software (version 1.40) was used for densitometric analysis.

Assessment of 5-Bromo-2-Deoxyuridine Incorporation. Mice received an intraperitoneal injection of 5-bromo-2-deoxyuridine (BrdU; 100 mg/kg; Roche Applied Science, Indianapolis, IN) 2 hours before sacrifice. Six random visual high-power fields (0.64 mm^2 per field) per mouse were evaluated to determine the number of BrdU-positive nuclei in hepatocytes and nonparenchymal cells. Nonparenchymal cells were defined as cells with smaller, irregularly shaped nuclei, compared with larger, circular nuclei of hepatocytes, as previously described.[14] All BrdU-positive cells, from both cell types, were summed at each time point.

Assessment of Apoptotic Index. Terminal deoxynucleotidyl transferase dUTP nick end labeling (TUNEL) analysis was performed using an *in situ* apoptosis detection kit (Roche). Six visual high-power fields (0.64 mm^2 per field) per mouse were evaluated to determine the number of TUNEL-positive nuclei.

Antibodies. The antibodies used for analyses are summarized in Supporting Table 1. The amount of active and total TGF-β1 in liver samples was determined using an enzyme-linked immunosorbent assay kit (Quantikine

Address reprint requests to: Takao Sakai, M.D., Ph.D., Department of Biomedical Engineering/ND20, Lerner Research Institute, Cleveland Clinic, 9500 Euclid Avenue, Cleveland, OH 44195. E-mail: sakait@ccf.org; fax: +01-216-444-9198.

View this article online at wileyonlinelibrary.com.

DOI 10.1002/hep.24800

Potential conflict of interest: Nothing to report.

Additional Supporting Information may be found in the online version of this article.

TGF-β1 Immunoassay; R&D Systems, Inc., Minneapolis, MN), according to the manufacturer's instructions.

Real-time Polymerase Chain Reaction. Real-time polymerase chain reaction (PCR) was performed as described previously.[13] The primers used are summarized in Supporting Table 2.

Lipid Peroxidation Assay. Liver tissue content of malondialdehyde (MDA) was measured by the thiobarbituric acid reduction method using a commercially available kit (#10009055; Cayman Chemical, Ann Arbor, MI). Values were obtained after 30-minute incubation at 90°C under acidic conditions.

In Vitro Assay Using Human Umbilical Vein Endothelial Cells and Mouse Primary Hepatocytes. Human umbilical vein endothelial cells (HUVECs) were used at passages 3-6. For analysis of reactive oxygen species (ROS), H_2O_2 (Thermo Fisher Scientific, Waltham, MA) and *N*-acetylcysteine (NAC; Calbiochem, San Diego, CA) were used as an ROS inducer and an ROS scavenger, respectively. To examine the effects of H_2O_2 on TSP-1 expression, HUVECs were seeded on 0.1% gelatin-coated culture plates and incubated overnight. Without change of medium, H_2O_2 was applied at final concentrations of 0.01, 0.05, and 0.1 mM and incubated for 10 minutes. For immunocytochemistry (ICC), HUVECs were plated into Lab-Tek Permanox slides precoated with 0.1% gelatin and incubated overnight. Then, the cells, with or without pretreatment with 30 mM of NAC for 60 minutes, were treated with 0.1 mM of H_2O_2 for 10 minutes.

To examine the effects of HUVEC-derived TSP-1 on TGF-β/Smad signaling and proliferation in primary hepatocyte cultures, primary hepatocytes were isolated from 8- to 12-week-old adult WT mouse livers using collagenase perfusion as previously described.[15] Isolated hepatocytes were plated on type I collagen (10-μg/mL)-coated dishes in Williams' E medium, supplemented with 5 μg/mL of insulin, 5 μg/mL of transferrin, 10 ng/mL of endothelial growth factor, 10^{-5} M aprotinin, 10^{-5} M of dexamethasone, 10^{-3} M of nicotinamide, and 10% fetal bovine serum and incubated at 37°C for 24 hours. To examine the effect of HUVEC-derived TSP-1 on TGF-β/Smad signaling in hepatocytes, the conditioned media from HUVECs (treated with 1.0 mM of H_2O_2 for 2 hours) were added to primary hepatocytes with or without pretreatment of 5 μM of LSKL or SLLK peptide (GenScript, Piscataway, NJ),[16,17] cultured for an additional 4 hours, and the cells were used for the analysis. To examine the effect of HUVEC-derived TSP-1 on hepatocyte proliferation, the conditioned media from HUVECs were added to primary hepatocytes, cultured for an additional 24 hours, and the cells were used for the analysis.

Data Presentation and Statistical Analysis. All experiments were performed in triplicate, and the data shown are representative of results consistently observed. Data are expressed as the mean ± standard deviation. Data analysis was performed with SPSS 12.0.1 for Windows (SPSS, Inc., Chicago, IL). Statistical analyses were performed using the Student *t* test or analysis of variance, followed by Bonferroni's multiple comparison tests, when appropriate. A *P* value of <0.05 was considered significant.

Results

PH Induces an Immediate and Prominent Induction of TSP-1 mRNA and Protein in the Regenerating Liver. An intact liver in adult mice expresses nearly undetectable levels of *TSP-1* mRNA.[12] We first determined whether PH could trigger TSP-1 induction in the regenerating liver. *TSP-1* mRNA was immediately induced, with a peak at 3 hours after hepatectomy, in WT mice by real-time PCR (Fig. 1A). TSP-1 protein was also induced, reaching a peak at ~6 hours (Fig. 1B). Those mRNA and protein levels returned to basal levels by 24 hours (Fig. 1A,B). Thus, PH induced immediate and transient TSP-1 expression in the initial phase of liver regeneration. Secondary minor inductions of *TSP-1* mRNA and protein were found to peak at 48 and 72 hours, respectively (Fig. 1A,B).

We next determined the cellular source of TSP-1 by immunostaining. In the intact liver, the expression of TSP-1 protein was detectable only in platelets with GPIIb/IIIa expression by double IF staining (Fig. 1C). The tissue distribution of TSP-1 protein localized in the sinusoid at 6 and 72 hours after PH (Fig. 1D), suggesting that cells localized in the sinusoid (e.g., endothelial cells [ECs], Kupffer cells, and hepatic stellate cells; HSCs) are responsible for newly synthesized TSP-1 in the regenerating liver. Double IF staining revealed that TSP-1 protein predominantly colocalized with platelet/endothelial cell adhesion molecule-1 (PECAM-1)/cluster of differentiation (CD)31 (an EC marker) at 6 hours in the regenerating liver (Fig. 2A). In contrast, TSP-1 protein at 6 hours did not colocalize with either F4/80 (a Kupffer cell marker) or alpha smooth muscle actin (α-SMA; a marker for myofibroblasts, such as activated HSCs) (Fig. 2A). The activation peak of HSCs is at 72 hours after PH[18] and many α-SMA-positive cells were observed (Supporting Fig. 1). At 72 hours, however, TSP-1 protein did

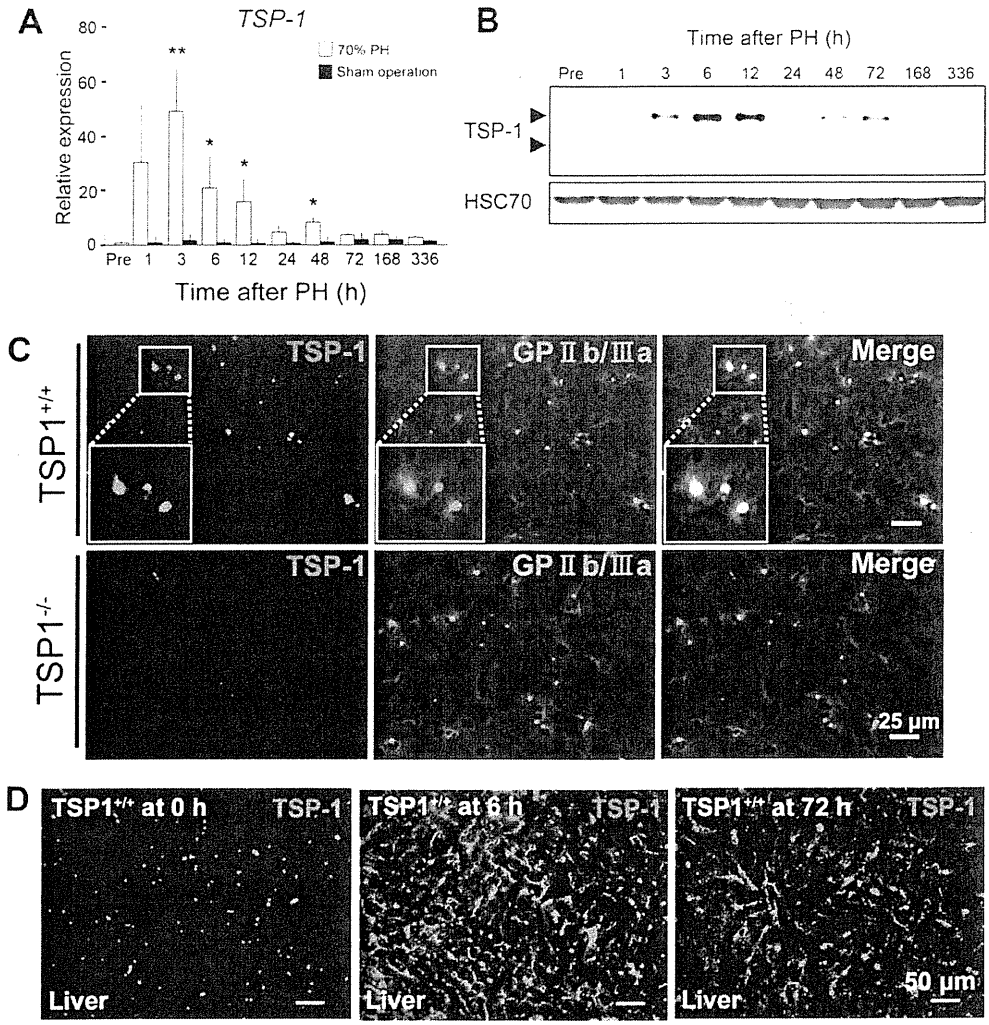

Fig. 1. An immediate and significant induction of *TSP-1* mRNA and protein in response to PH. (A) Real-time PCR analysis of *TSP-1* mRNA expression after 70% PH (n = 8 per time point) versus sham operation (n = 3 per time point). Data were normalized to the amount of *18S ribosomal* RNA serving as the internal control. $^{*}P < 0.05$ versus sham-operated mice; $^{**}P < 0.01$ versus sham-operated mice. (B) Western blotting analysis of TSP-1 protein expression in the regenerating liver. Heat shock cognate protein 70 (HSC70) served as a loading control. (C) Double IF staining of TSP-1 (red) and GPIIb/IIIa (green) at 0 hours in WT ($TSP1^{+/+}$) and TSP-1-null ($TSP1^{-/-}$) liver. Note that the distribution of TSP-1 in the intact WT liver shows only in platelets, as evidenced by colocalization of TSP-1 with the platelet marker, GPIIb/IIIa (yellowish dots in the merged image). Scale bar = 50 μm. (D) IF staining for TSP-1 in WT liver at 0, 6, and 72 hours after PH. Scale bar = 50 μm.

colocalize with PECAM-1/CD31 and α-SMA, but not with F4/80 (Fig. 2B). Indeed, it is known that activated HSCs express TSP-1 and thereby activate the TGF-β-signaling pathway *in vitro*.[19] These results suggest that ECs are the major source of TSP-1 expression in the initial phase at 6 hours, whereas ECs and activated HSCs participate in secondary TSP-1 expression at 72 hours. As noted above, immediate early genes are genes that are rapidly, but transiently (within approximately the first 4 hours), activated in response to hepatectomy.[1,2] Thus, TSP-1 produced by ECs is a novel candidate immediate early gene in the initial response to PH.

TSP-1 Deficiency Accelerates a Liver Regeneration After PH, but Does Not Affect the Termination Phase. Because immediate early genes play a significant role in the regulation of cell growth in the regenerating liver,[1,2] we next examined the involvement of TSP-1 in the control of liver regeneration. The rates of recovery of liver mass and of cell proliferation after PH were compared between WT and TSP-1-null mice. TSP-1-null mice showed significantly faster recovery of liver:body-weight ratio from day 1 to day 7 after surgery, compared with controls ($P < 0.05$ at 24, 48, and 168 hours and $P < 0.01$ at 72 hours; Fig. 3A). However, no excess liver mass had been gained at day

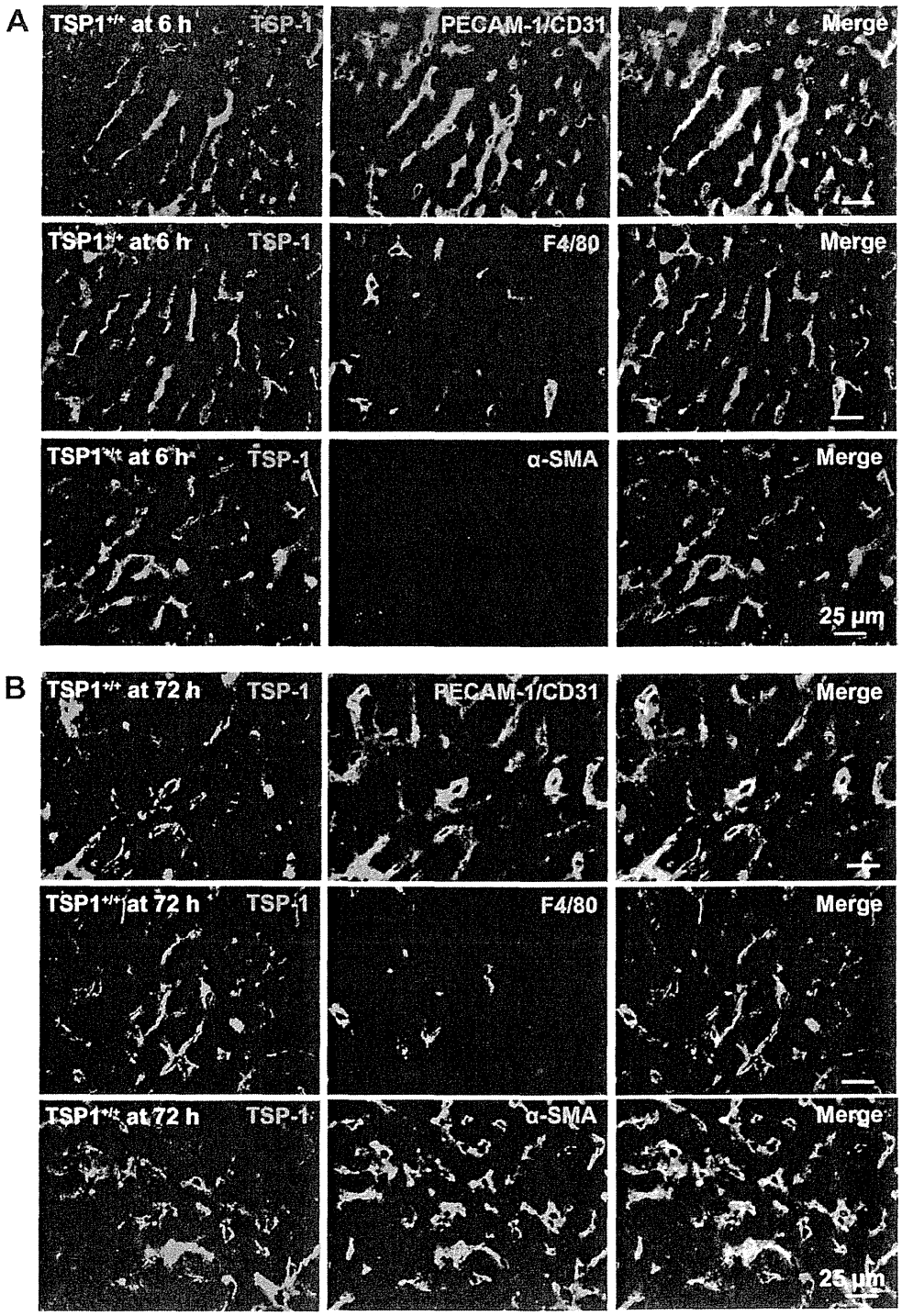

Fig. 2. Tissue distribution of TSP-1 protein in the regenerating liver. (A and B) TSP-1 expression at 6 (A) and 72 hours (B) after PH. Double IF staining for TSP-1/PECAM-1 (CD31), TSP-1/F4/80, and TSP-1/α-SMA at 6 and 72 hours in WT mice (TSP-1, red; PECAM-1 [CD31], F4/80, and α-SMA, green). Scale bar = 25 μm.

14 in TSP-1-null mice, compared with controls. Next, cell proliferation was evaluated using a BrdU incorporation assay (a marker for the S phase of the cell cycle). The proliferation peaks of hepatocytes and nonparenchymal cells after PH occurred at ~36-48 and 72 hours, respectively.[2,4,14] Although only a few

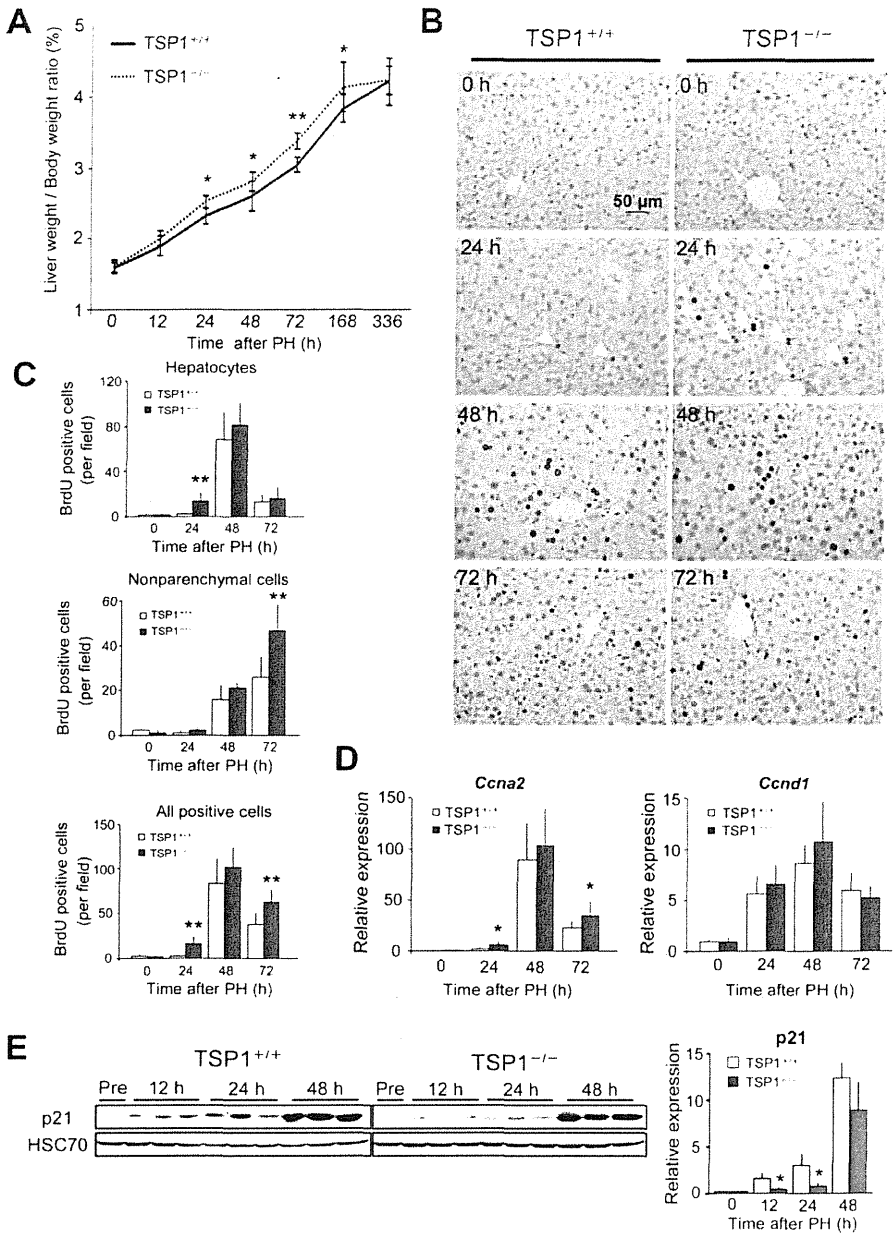

Fig. 3. Accelerated liver regeneration with down-regulation of p21 protein expression in TSP-1-null mice after PH. (A) Assessment of restoration of liver mass. Liver:body-weight ratio was measured after PH (n = 10 per time point in each group). *$P < 0.05$ versus *TSP-1*$^{+/+}$ mice; **$P < 0.01$ versus *TSP-1*$^{+/+}$ mice. (B and C) Assessment of BrdU incorporation in the regenerating liver. (B) IHC of BrdU in the regenerating liver. Arrowheads indicate BrdU-positive hepatocyte nuclei (brown) at 24 hours. Scale bar = 50 μm. (C) The number of BrdU-positive hepatocytes, nonparenchymal cells, and all positive cells (n = 10 per time points in each group). **$P < 0.01$ versus *TSP-1*$^{+/+}$ mice. (D) Real-time PCR analysis of *cyclin A2* (*Ccna2*) and *cyclin D1* (*Ccnd1*) mRNA expression in the regenerating liver (n = 10 per time point in each group). *$P < 0.05$ versus *TSP-1*$^{+/+}$ mice. (E) Assessment of p21 protein expression in the regenerating liver. Left panels: western blotting analysis of *p21 protein expression in WT versus TSP-1-null liver. HSC70 was used as a loading control.* Right panel: *densitometric analysis of p21 protein* expression (n = 3). Each p21 intensity was normalized to HSC70, then the intensity of WT mice at 0 hours was set to 1. *$P < 0.05$ versus *TSP-1*$^{+/+}$ mice. HSC70, heat shock cognate protein 70.

BrdU-positive hepatocytes were detectable at 24 hours in WT mice, TSP-1-null mice showed a significantly increased number of BrdU-positive hepatocytes (8-fold over controls) ($P < 0.01$; Fig. 3B,C). The number of BrdU-positive nonparenchymal cells in TSP-1-null mice significantly increased (2-fold) at 72 hours, compared with controls ($P < 0.01$; Fig. 3C). Total proliferative activity (of hepatocytes and

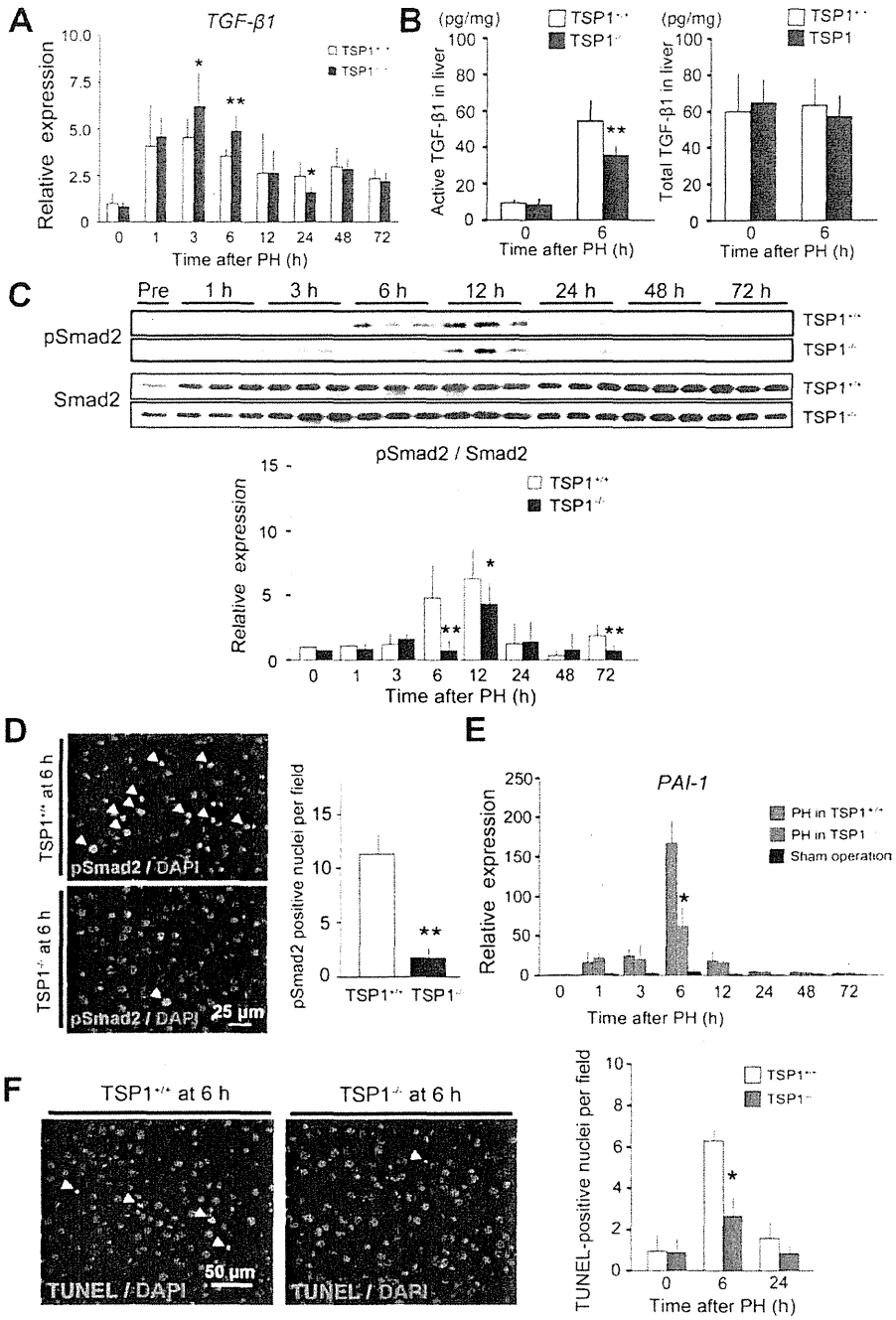

Fig. 4. Significantly decreased TGF-β/Smad signal transduction and cell death in TSP-1-null mice after PH. (A) Real-time PCR analysis of *TGF-β1* mRNA expression after PH (n = 8 per time point in each group). $*P < 0.05$ versus *TSP-1*$^{+/+}$ mice; $**P < 0.01$ versus *TSP-1*$^{+/+}$ mice. (B) Levels of active and total TGF-β1 in WT and TSP-1-null liver at 6 hours after PH (n = 6 per time point in each group). $**P < 0.01$ versus *TSP-1*$^{+/+}$ mice. (C-E) Effects of TSP-1 deficiency on pSmad2 expression in the regenerating liver. (C) Upper panels: western blotting analysis of pSmad2 and total Smad2 in WT and TSP-1-null liver. Lower panel: densitometric analysis of pSmad2 protein expression (n = 3). Each pSmad2 intensity was normalized to total Smad2, then the intensity of WT mice at 0 hours was set to 1. $*P < 0.05$ versus *TSP-1*$^{+/+}$ mice; $**P < 0.01$ versus *TSP-1*$^{+/+}$ mice. (D) Assessment of pSmad2 nuclear localization. Left panel: IF staining for pSmad2 at 6 hours in WT and TSP-1-null liver. Right panel: analysis of pSmad2-positive nuclei (n = 5 in each group). Arrowheads indicate pSmad2 (red)/ DAPI (blue) double-positive nuclei (purple). $**P < 0.01$ versus *TSP-1*$^{+/+}$ mice. Scale bar = 25 μm. (E) Real-time PCR analysis of *PAI-1* mRNA expression in WT and TSP-1-null liver after PH (n = 8 per time point in each group) and in WT liver after sham operation (n = 3 per time point). $**P < 0.01$ versus *TSP-1*$^{+/+}$ mice. (F) Assessment of TUNEL-positive cell death in the regenerating liver. Left panel: TUNEL staining at 6 hours after PH in WT and TSP-1-null liver. Right panel: analysis of TUNEL-positive cells (n = 5 per time point in each group). Arrowheads indicate TUNEL (red)/DAPI (blue) double-positive nuclei (purple). $**P < 0.01$ versus *TSP-1*$^{+/+}$ mice. Scale bar = 50 μm. DAPI, 4′,6-diamidino-2-phenylindole.

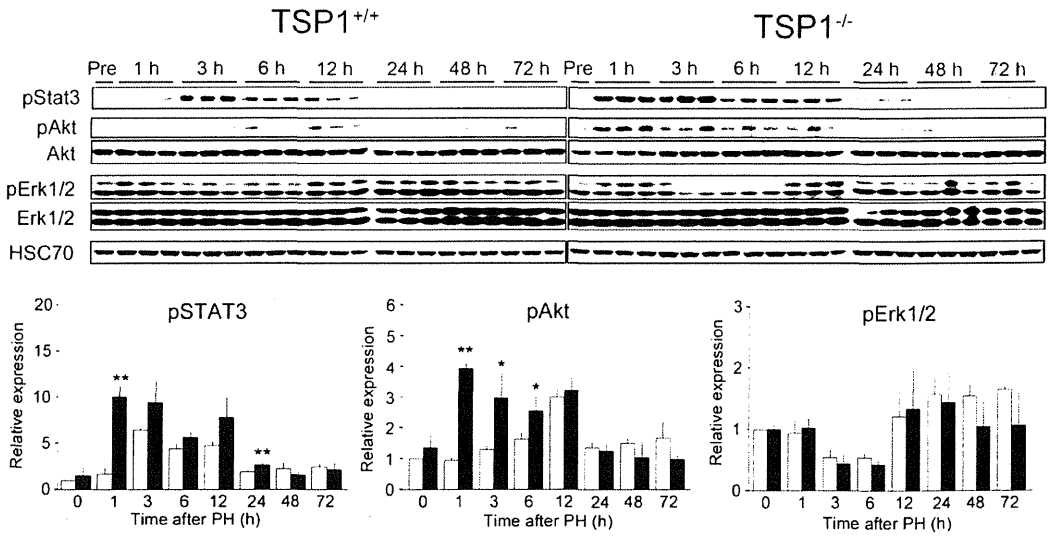

Fig. 5. TSP-1 deficiency enhances STAT3 and PI3K/Akt, but not Erk1/2 signal, in the early phase after PH. Upper panels: western blotting analysis of STAT3, PI3K/Akt, and Erk1/2 signals. HSC70 served as a loading control. Lower panels: densitometric analysis of phosphorylated protein expression after PH. Each pSTAT3, pAkt, and pErk1/2 intensity was normalized to HSC70, then the intensity of WT mice at 0 hours was set to 1. $*P < 0.05$ versus *TSP-1*$^{+/+}$ mice; $**P < 0.01$ versus *TSP-1*$^{+/+}$ mice.

nonparenchymal cells) in TSP-1-null mice was significantly higher at 24 and 72 hours, compared with controls ($P < 0.01$ in both; Fig. 3C).

Cyclins are required for cell-cycle progression. The mRNA levels of cyclin A2 (*Ccna2*) and cyclin D1 (*Ccnd1*) increase and peak in S phase and early to mid G_1 phase, respectively. Expression levels of *Ccna2* mRNA in TSP-1-null mice were significantly higher at 24 (2.3-fold) and 72 hours (1.5-fold), compared with controls ($P < 0.05$ in both; Fig. 3D). Although *Ccnd1* mRNA levels increased and peaked at 48 hours in both WT and TSP-1-null mice, there was no significant difference between them (Fig. 3D). The cyclin-dependent kinase inhibitor, p21, plays a critical role in the inhibition of hepatocyte proliferation at the G_1/S transition of the cell cycle *in vivo*.[20] Induction levels of p21 protein in TSP-1-null mice significantly diminished at 12 and 24 hours, compared with controls (70% less than that of controls, both at 12 and 24 hours; $P < 0.05$ in both), whereas p21 showed at similar levels at 48 hours in WT and TSP-1-null liver (Fig. 3E). These results suggest that TSP-1 is a negative regulator of liver regeneration after PH, and that TSP-1 deficiency accelerates the S-phase entry of hepatocytes by down-regulation of p21 protein expression. However, TSP-1 does not affect the termination phase of liver regeneration after PH.

TGF-β/Smad Signaling Is Activated by TSP-1 in Response to PH. To address the possible mechanisms underlying this accelerated liver regeneration in TSP-1-null mice, we examined TGF-β/Smad signaling. *TGF-β1* mRNA levels in both WT and TSP-1-null mice increased after hepatectomy by real-time PCR, and those levels in TSP-1-null mice were significantly up-regulated at 3 and 6 hours, compared with controls ($P < 0.05$ at 3 hours and $P < 0.01$ at 6 hours; Fig. 4A). In sharp contrast, the levels of active TGF-β1 in TSP-1-null liver were significantly lower than controls at 6 hours after PH, whereas the levels of total TGF-β1 did not show any significant differences between them (Fig. 4B). Furthermore, the levels of phosphorylated Smad2 (pSmad2, C-terminal Ser465/467) protein, as a downstream mediator of active TGF-β1, significantly diminished at 6 and 12 hours in TSP-1-null mice, compared with controls (to 16% at 6 hours and 69% at 12 hours versus controls, respectively; $P < 0.01$ at 6 hours and $P < 0.05$ at 12 hours), as determined by western blotting (Fig. 4C). Using IF staining, we confirmed the significantly decreased number of nuclear localized pSmad2-positive cells at 6 hours in TSP-1-null mice, compared with controls ($P < 0.01$; Fig. 4D). A secondary, minor induction of pSmad2 at 72 hours was also significantly attenuated in TSP-1-null mice, compared with controls (Fig. 4C).

Plasminogen activator inhibitor-1 (PAI-1) is one of the downstream targets of TGF-β1 in hepatocytes.[21] Although intense inductions of *PAI-1* mRNA at 6 hours after hepatectomy were observed in both WT mice and TSP-1-null mice by real-time PCR, the induction level in TSP-1-null mice was significantly diminished (to 37% of controls; $P < 0.05$ at 6 hours) (Fig. 4E).

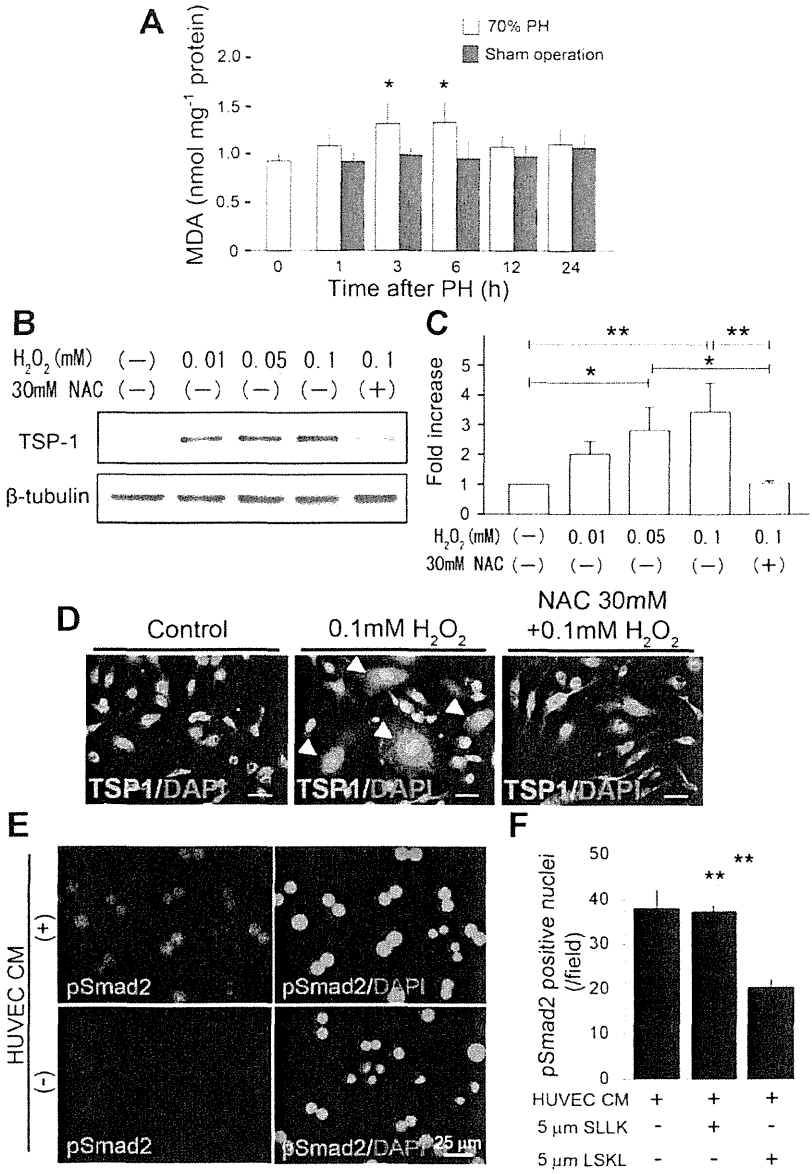

Fig. 6. TSP-1 induction in ECs by ROS. (A) Assessment for levels of MDA after 70% PH (n = 5) and sham operation (n = 3). *P < 0.05 versus sham-operated mice. (B-D) TSP-1 protein expression by H_2O_2, a potent ROS inducer, in HUVECs. (B) Western blotting analysis of TSP-1 after treatment of HUVECs with H_2O_2. β-tubulin served as a loading control. (C) Densitometric analysis of TSP-1 expression from three independent experiments. Each TSP-1 intensity was normalized to β-tubulin, then the intensity of control was set to 1. Note that the TSP-1 protein expression levels after treatment with 0.05 and 0.1 mM of H_2O_2 are significantly higher versus controls, whereas the induction of TSP-1 by treatment with 0.1 mM of H_2O_2 is significantly inhibited with a pretreatment using 30 mM of NAC. *P < 0.05; **P < 0.01. (D) ICC for TSP-1 protein in HUVECs after treatment with H_2O_2 (TSP-1, green; DAPI, blue). Note that HUVECs after treatment with 0.1 mM of H_2O_2 express TSP-1 in their cytoplasm (arrowheads), whereas the induction of TSP-1 is inhibited by pretreatment using 30 mM of NAC. Scale bar = 50 μm. (E and F) Assessment of pSmad2 nuclear localization in primary hepatocytes. (E) IF staining for pSmad2 with or without ROS-treated CM from HUVECs (HUVEC CM). Scale bar = 25 μm. (F) Effect of TSP-1-inhibitory peptide LSKL on pSmad2 induction. Error bars represent standard deviation (n = 5 in each group; field = 0.15 mm^2). SLLK, control peptide. **P < 0.01. DAPI, 4′,6-diamidino-2-phenylindole.

Cell death is also implicated as a mechanism of TGF-β-mediated cell-growth inhibition. TUNEL-positive cells, as a marker for cell death, are immediately and transiently detectable after hepatectomy.[22] We determined whether deficiency in TSP-1 affected cell death in the regenerating liver. Although the number of TUNEL-positive cells in WT liver transiently increased at 6 hours after hepatectomy, TSP-1-null liver showed a significant reduction, compared with controls (P < 0.05 at 6 hours; Fig. 4F).

These results suggest that TSP-1-mediated active TGF-β1 plays a pivotal role in TGF-β/Smad signal transduction after PH.

Deficiency in TSP-1 Accelerates STAT3 and PI3K/Akt Signals, Not Extracellular Signal-Related Kinase 1 And 2 Signal, in the Early Phase After PH. There is *in vitro* evidence that TSP-1 down-regulates phosphorylated Akt (Ser473) expression through its receptor, CD47, in HUVECs.[23] Indeed, signaling pathways, such as phosphatidylinositide 3-kinase (PI3K)/Akt, signal transducer and activator of transcription 3 (STAT3), and extracellular signal-related kinase 1 and 2 (Erk1/2), are important for cell survival and/or proliferation after PH.[24] Therefore, we next examined whether the deficiency in TSP-1 affected the activation of these signaling pathways in the early phases po

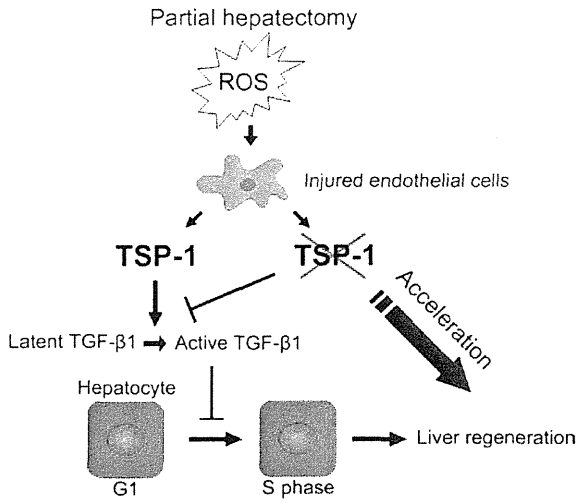

Fig. 7. Schematic illustration of the role of TSP-1 in the regenerating liver. In WT mice, newly synthesized ROS in response to PH stimulate ECs to express TSP-1. TSP-1 induced by ECs converts latent TGF-β1 into its active form. Active TGF-β1 suppresses cell-cycle progression in hepatocytes at the G_1/S checkpoint. In contrast, TSP-1 deficiency decreases active TGF-β1 levels, which, in turn, results in the acceleration of liver regeneration.

hepatectomy. TSP-1-null mice showed earlier, more intense phosphorylation of STAT3 (Tyr705) (6-fold at 1 hour; $P < 0.01$) and Akt (Ser473) (4.2-fold at 1 hour; $P < 0.01$) in the early stage after PH, compared with controls, as determined by western blotting (Fig. 5). In contrast, levels of phosphorylated Erk1/2 did not show any remarkable differences between the two groups (Fig. 5).

TSP-1 Induction in ECs Is Associated With ROS. Although our findings show that TSP-1 plays a potential role as a negative regulator in the regenerating liver, the mechanism of TSP-1 induction in ECs in response to PH remains unknown. There is a line of evidence that ROS are produced in the regenerating liver after PH.[22,25] In WT mice, levels of tissue content of MDA as a lipid peroxidation marker for ROS generation were significantly increased at both 3 and 6 hours and returned to basal levels by 12 hours after hepatectomy ($P < 0.05$ in both; Fig. 6A). Next, to determine whether ROS could induce TSP-1 expression in ECs, we performed an *in vitro* study using HUVECs with the potent ROS inducer, H_2O_2. In HUVECs, treatment with H_2O_2 induced TSP-1 protein expression in a dose-dependent manner (Fig. 6B-D). Furthermore, this induction was inhibited by pretreatment with 30 mM of NAC, a scavenger of ROS (Fig. 6B-D). Thus, these results indicate that oxidative stress is one factor responsible for TSP-1 induction in ECs.

To further determine whether HUVEC-derived TSP-1 could modulate TGF-β/Smad signaling and proliferation in hepatocytes *in vitro*, we isolated primary hepatocytes from adult WT mice.[15] The treatment of conditioned media from HUVECs with primary hepatocytes actually induced pSmad2 (Fig. 6E). Furthermore, the pretreatment of primary hepatocytes with TSP-1-inhibitory peptide LSKL[16,17] significantly suppressed conditioned media (CM)-induced pSmad2 expression, whereas the control peptide, SLLK, showed no effects (Fig. 6F). It is known that primary hepatocytes lack the ability to proliferate, even though such cells *in vivo* readily replicate and/or synthesize DNA after PH.[26] Although a few proliferative primary hepatocytes were found by Ki67 immunostaining in culture, the treatment of CM from HUVECs with primary hepatocytes significantly reduced the number of Ki67-positive cells (Supporting Fig. 2).

Discussion

In the present study, we have demonstrated the following (Fig. 7): (1) TSP-1 is induced in ECs as an immediate early gene by ROS and participates in TGF-β signal transduction in the initial response to PH and (2) TSP-1 deficiency results in the significant reduction of TGF-β/Smad signal, and this could cause the accelerated S-phase entry of hepatocytes by down-regulation of p21 protein expression. Thus, this is the first study providing compelling evidence that local TGF-β activation machinery plays an important role in inhibiting liver regeneration after PH.

Our study supports the notion that oxidative stress is one factor responsible for TSP-1 induction in the regenerating liver. TSP-1 is the most likely candidate protein induced by oxidative stress in proteomic analysis using brain ECs.[27] These findings imply that ECs initially sense locally produced ROS in response to tissue damage, and that the subsequent induction of TSP-1 in these cells after initiates tissue remodeling. Indeed, our results revealed that EC-derived TSP-1 can modulate TGF-β/Smad signaling and proliferation in hepatocytes. ECs represent the largest population of nonparenchymal cells in the liver. Identification of the functional role of immediate early genes provides the clues for understanding the molecular bases of liver regeneration. One recent study documented that Id-1, a vascular endothelial growth factor-A receptor (VEGFR)-2-mediated transcriptional factor, was induced in ECs at ~48 hours after hepatectomy; Id-1, in turn, promoted hepatocyte proliferation.[28] There has, as yet, been no report implicating ECs in earlier

stages of the regenerating liver (within 24 hours). We have identified TSP-1 as a novel immediate early gene derived from ECs, showing that the expression level of TSP-1 was immediately up-regulated and returned to basal levels by 24 hours in response to PH. Our findings and the previous report[28] suggest that ECs may play two distinct roles in hepatocyte proliferation after PH: One is an antiproliferative role by activating the TSP-1/TGF-β1 axis within 24 hours, and the other is a proproliferative role by activating VEGFR-2 after 24 hours. This finding is consistent with the evidence that TSP-1 inhibits the activation of VEGFR-2 through its receptor, CD47, in ECs,[23] and suggests that the reduction of TSP-1 expression may be required for the functional shift in ECs from an anti- to a proproliferative role in hepatocytes. Microvascular rearrangement is important for tissue remodeling, and the antiangiogenic action is one of the well-recognized functions of TSP-1.[29] However, the expression of CD31 mRNA for monitoring angiogenesis did not show any significant difference between WT and TSP-1-null mice at 24, 48, and 72 hours after PH (Hayashi H, and Sakai T; unpublished data), suggesting that TSP-1 does not affect vascularization during liver regeneration after PH.

TGF-β1 is known to be a potent inhibitor of mitogen-stimulated DNA synthesis in cultured hepatocytes.[3] p21 is important for inhibiting hepatocyte proliferation *in vivo*, especially at the G_1/S transition of the cell cycle,[20] and the expression of p21 is up-regulated by TGF-β1.[30] There is evidence that *TGF-β1* mRNA induction occurs within 4 hours and remains elevated until 72 hours after PH.[5,6] In contrast, we found the only limited activation of TGF-β signaling in an earlier phase (within 24 hours), with a peak at ~12 hours. It is known that TGF-β is secreted as latent forms and they are converted into active TGF-β in response to injury. There are several mechanisms for activation, such as by proteases, integrins (e.g., $\alpha v\beta 6$ and $\alpha v\beta 8$), and TSP-1, all of which are likely to be tissue specific.[31] Whereas the complete lack of TGF-β-mediated signal in hepatocyte-specific *TGF-β type II receptor* knockout mice accelerates hepatocyte proliferation in the later phase (~36-48 hours) after hepatectomy,[7] the role of TGF-β signaling in the earlier phase (within 24 hours) remains to be elucidated. Our present findings provide compelling evidence that locally activated TGF-β1 mediated by TSP-1 as an immediate early gene is critical in the early phase (within 24 hours) post PH to initiate the inhibitory effect on hepatocyte proliferation, and this TGF-β signaling has a functional link to the G_1/S-phase transition by modulating p21 protein expression. A major downstream target of TGF-β1, PAI-1,[21] is a negative regulator of liver regeneration, and PAI-1-null mice show acceleration of liver regeneration after Fas-mediated massive hepatocyte death.[32] The significant down-regulation of PAI-1 expression in our TSP-1-null liver may be implicated in the accelerated hepatocyte proliferation after PH. However, our TSP-1-null model did not show any obvious differences in the termination phase of liver regeneration, compared with controls, such as the *TGF-β type II receptor* knockout mice model.[7] Although the molecular mechanisms underlying the termination of liver regeneration remain to be elucidated,[4] our and other findings suggest that the orchestrating interactions among positive and negative regulators in hepatocyte proliferation would be critical for the termination of liver regeneration.[4,24]

Active TGF-β1 induces hepatocyte cell death. STAT3- and PI3K/Akt-signaling pathways are crucial for cell survival (i.e., antiapoptosis) in the acute phase after PH. Our signaling data using TSP-1-null mice are consistent with previous findings showing that STAT3- and PI3K/Akt-signaling pathways, but not the Erk1/2 pathway, play a protective role against TGF-β-induced apoptosis in hepatocyte cell lines.[33,34] Several *in vitro* studies have reported that TSP-1 down-regulates phosphorylated Akt expression in retina[35] and ECs.[23] Another *in vitro* study showed that the lack of TSP-1 in retinal ECs results in up-regulation of phosphorylated Akt expression, but not phosphorylated Erk1/2.[36] Because TSP-1 is a multidomain and multifunctional matricellular protein, our data and these findings suggest that TSP-1 modulates not only TGF-β signal, but also cell survival signals, such as STAT3 and PI3K/Akt signals, through its multidomain.

In the clinical setting, no established therapeutic strategies to accelerate liver regeneration have been available, to date. The inhibition of TSP-1 function attenuates locally activated TGF-β1 signals and thereby accelerates hepatocyte proliferation; hence, TSP-1 could be a novel therapeutic target for accelerating liver regeneration after PH.

Acknowledgments: The authors thank Dr. Jack Lawler for TSP-1-null mice, Drs. Koichi Matsuzaki and Deane Mosher for antibodies, and Diskin Erb and Dr. Judy Drazba (Imaging Core, Lerner Research Institute, Cleveland, OH) for IF microscopic analyses. The authors are also grateful to Dr. Jo Adams for assistance with TSP-1 immunostaining experiments and scientific discussions.